Critical Reviews in Biochemistry and Molecular Biology, 26(1):77—127 (1991)

Comparative Modeling of Proteins in the Design of Novel Renin Inhibitors

Charles Hutchins and Jonathan Greer

Computer Assisted Molecular Design Group, Pharmaceutical Products Division, Abbott Laboratories, Abbott Park, Illinois

Referee: Dennis J. Hoover, Dept. of Medicinal Chemistry, Pfizer Inc., Central Research Division, Groton, CT 06340

ABSTRACT: Renin, the first enzyme in the renin-angiotensin system, is critically important for the maintenance of blood pressure, and, therefore, as a target for antihypertensive therapy. The three-dimensional structure of renin would be an invaluable aid in understanding the functional properties of renin as well as in the design of novel, potent inhibitors. Three-dimensional models of renin have been developed by a number of different groups based on comparative homology modeling from the other known aspartic proteinase structures. These models have been used widely in the drug design process to suggest targets for synthesis and to rationalize the structure-activity relationships of compounds. This review describes the different published renin models and compares them to the extent possible. Applications of these model renin and renin-inhibitor complex structures to biological function and inhibitor design are summarized.

KEY WORDS: renin-angiotensin system, renin inhibitors, antihypertensive agents, comparative homology modeling, three-dimensional structure.

I. INTRODUCTION

One of the major blood pressure control pathways in the body involves the renin-angiotensin system (Figure 1). In this pathway, the first enzyme, renin, cleaves angiotensinogen, a large protein found in the blood, to produce a decapeptide called angiotensin I. Angiotensin I is further cleaved by angiotensin-converting enzyme (ACE) to produce angiotensin II, an octapeptide that is one of the most potent pressor molecules in the body. These two enzymes have received considerable attention because of the critical role they play in maintaining blood pressure and as targets of antihypertensive therapy. In particular, the ACE inhibitors have become highly successful antihypertensive agents,[1] and there is considerable promise that the renin inhibitors will be highly effective as well.[2]

A vast literature exists for renin itself.[2] In this review, we will focus on the role that modeling of the three-dimensional structure of renin has played in our understanding of the function and properties of this important enzyme. In addition, we will summarize the efforts that have been made to use these three-dimensional models of the renin molecule to aid in drug-design efforts.

Over the past 6 years or so, a variety of groups have reported the construction of models of human renin (Table 1) using comparative modeling methods.[3-9] Remarkably, most of these groups have approached the modeling from different perspectives. First we will summarize the models that have been produced. We will attempt

1040-9238/91/$.50

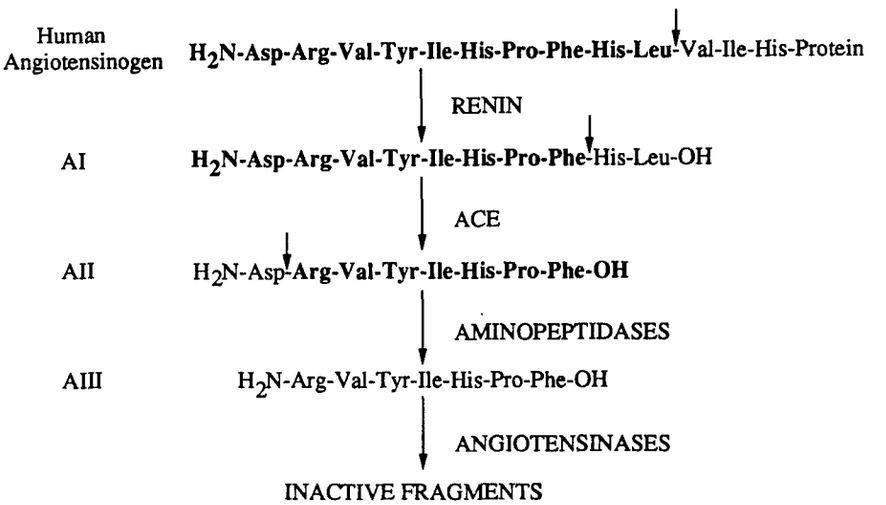

FIGURE 1. Schematic of the renin-angiotensin system.

TABLE 1
Models of Renin Reported

Group	Structure used to build	Species built	Date	Ref.
Blundell/Pfizer	Endothiapepsin	Human/ mouse	1984 1983	45 44
Carlson	Rhizopuspepsin	Human/ mouse	1985 1984	49, 50 54
Akahane/Kissei	Rhizopuspepsin	Human	1985	55
Raddatz/E. Merck	Penicillopepsin	Human	1985	62
Merck	Rhizopuspepsin[a]			
Abbott-original	Pepsin[b], Penicillo-, Rhizopus-, Endothiapepsin	Human/mouse	1986	35, 36
Abbott-new	Pepsin[c], chymosin, Penicillo-, Rhizopus-, endothiapepsin	Human	1989	37

[a] Inhibitor modeling was performed by analogy to the rhizopuspepsin structure and not from a constructed renin structure.
[b] Partially refined structure obtained from Andreeva.[59]
[c] Fully refined structure of pepsin.[64]

to describe differences between them to the extent possible from the published material. We will conclude with a summary of the applications that have ensued from the study of these model structures, both to improve our understanding of how this enzyme works and also to help in the design of potent inhibitors.

An introduction to modeling of the three-dimensional structure of renin would not be complete without discussing the state of crystalliza-

tion efforts on renin. The lack of significant amounts of human renin caused an early focus on crystallizing the much more easily prepared mouse submaxillary gland renin. Crystallization of this renin was reported several years ago[10]; however, this structure has not been solved to date because of the poor quality of the crystals. More recently, major efforts were instituted to clone and express human renal renin in large quantities for the purpose of performing structural studies.[11] Such efforts have succeeded with the publication this past year of the crystal structure of human renin by James and his co-workers.[12] However, since the coordinates for this structure have not yet been made available to the scientific community, we are unable to provide a detailed comparison between this experimentally determined structure and the models that were published previously. Some comments will be made based upon the figures published in the crystal structure paper.

II. MODEL STRUCTURES

A. Structure of the Aspartic Proteinase Family

Early studies on the enzyme renin determined that it was a member of the well-known aspartic proteinase family. The fact that it is inhibited by the classic aspartic proteinase inhibitor, pepstatin,[13] albeit much more weakly than is pepsin, was a clear indication that it is a member of this family.[14,15]

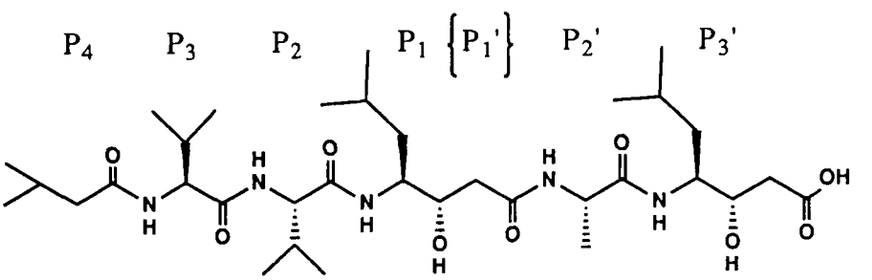

Pepstatin = Isovalyl-valyl-valyl-statyl-alanyl-statine

Determination of the sequence, first of mouse submaxillary gland renin[16,17] and then of human renin,[11,18-21] proved definitively that renin is a full-fledged member of this family of proteins. Once this fact was confirmed and the sequence of renin became available, the methods of comparative modeling[3-9] could be applied to construct three-dimensional model structures for renin based upon the known structures for other members of the aspartic proteinase family.

In order to appreciate the challenges involved in modeling the structure of renin, it is useful to begin by reviewing the structure and sequence information available for the aspartic proteinases. Table 2 provides a summary of the known experimental structures and sequences for this family. Since this information has been accumulating during the course of the past 6 to 7 years, the approximate date when the respective information was published is indicated. A comparison of the dates in this table with those in Table 1 will indicate approximately which pieces of information were available to each group performing the respective modeling study.

The structures of the three fungal enzymes are shown superimposed in Figure 2. These structures have provided the structural information for virtually all the modeling efforts on renin that have been reported (Table 1). It can be seen that the structures agree quite closely, i.e., are structurally conserved, for large parts of the molecule. There are, however, regions of quite variable conformation scattered throughout the molecule that are composed primarily of the external loops of the molecule. Figure 3 shows an alignment of the sequences for these three proteins based upon the above correspondence of their three-dimensional structures. Also aligned in Figure 3 are the sequences of porcine pepsin,[22] bovine chy-

TABLE 2
Structures and Sequences of the Aspartic Proteinases

Protein	3D structure date-resolution	Ref.	Sequence date	Ref.
Fungal enzymes				
Penicillopepsin	1983—1.8 Å	56		
Rhizopuspepsin	1982—2.5 Å	26	1987[a]	52
Endothiapepsin	1984—2.1 Å	46	1987[a]	113
Mammalian enzymes				
Pepsin	1984—2.0 Å[b]	59	1973	22
	1990—2.0 Å[c]	64		
Chymosin	1990—2.3 Å	65	1979	23
Cathepsin D	Not yet		1984	114
Mouse renin	Not yet		1982	16, 17
Human renin	1989—2.5 Å[d]	12	1983	11, 18-21

[a] Crystallographically derived sequences were available earlier with the original high-resolution structures. However, these sequences tend to have many errors.
[b] The partially refined coordinates of this structure were obtained from Dr. Andreeva and were not generally available.
[c] A highly refined structure of pepsin is now available as of 1990.[64]
[d] Coordinates will not be available for at least 1 year.

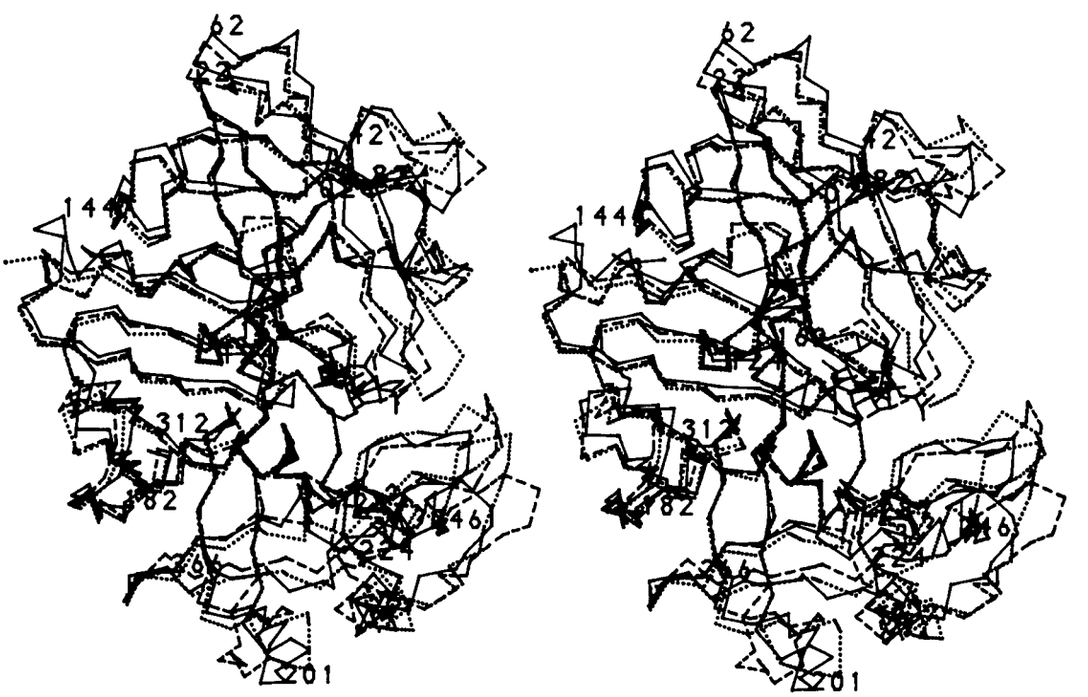

FIGURE 2. Overlap of the three fungal aspartic proteinase structures: endothiapepsin (4APE, dotted), penicillopepsin (2APP, dashed), and rhizopuspepsin (solid). The substrate/inhibitor binding site is marked by pepstatin as it is complexed to rhizopepsin.[26] Coordinates for the crystal structures were obtained from the Brookhaven Protein Structure Data Base.[115]

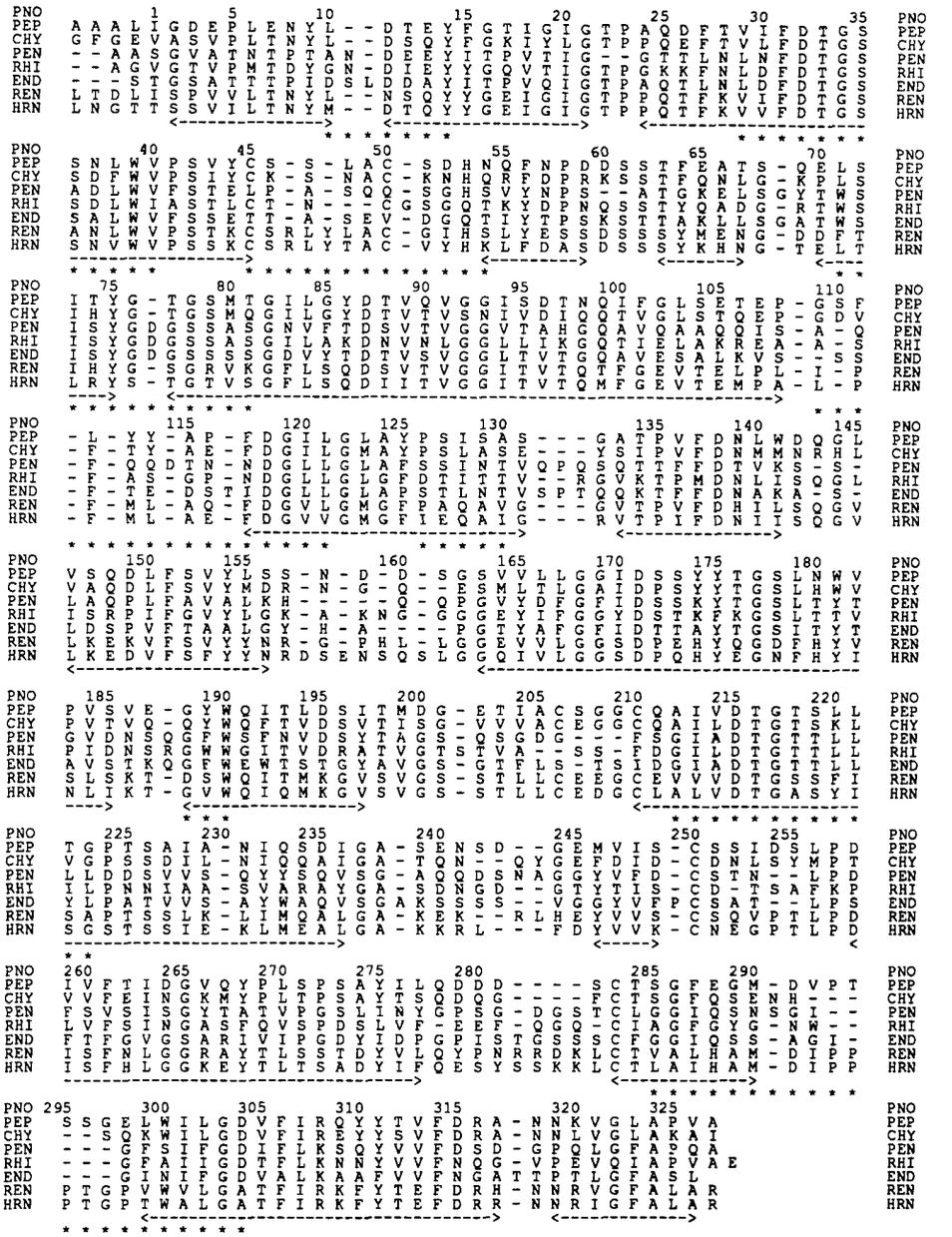

FIGURE 3. Alignment of the aspartic proteinase sequences based upon the three-dimensional structure alignment. The line labeled *PNO* gives the pepsin residue numbering used throughout this review. The sequences are labeled as follows: PEP = porcine pepsin, CHY = bovine chymosin, PEN = penicillopepsin, RHI = rhizopuspepsin, END = endothiapepsin, REN = mouse renin, HRN = human renin. The sequences for the proteins with crystal structures were aligned based upon the superposition of the three-dimensional structures. The remaining proteins were aligned based upon homology as previously described.[6,9,36] The IUPAC-IUB convention, standard single-letter amino-acid code used in this figure is as follows: A = Ala, C = Cys, D = Asp, E = Glu, F = Phe, G = Gly, H = His, I = Ile, K = Lys, L = Leu, M = Met, N = Asn, P = Pro, Q = Gln, R = Arg, S = Ser, T = Thr, V = Val, W = Trp, Y = Tyr. Position of relative deletions in the sequences are denoted by a "−". The ←---→ symbols delineate the structurally conserved regions of the molecule.[6,9,36] The * indicate those residues that are close to the substrate/inhibitor binding site.

mosin,[23] and both mouse[16,17] and human[11,18-21] renins. While there are some differences in the way the different groups have aligned the human renin sequence to the other aspartic proteinases, the differences are relatively minor and are not critical to the overall analysis of the aspartic proteinase structures described here. These differences, when important, will be described in the next section, which details the various published models.

The fungal aspartic proteinase structures (Figure 2) show that the molecule is composed of two domains, a N-terminal and a C-terminal domain. The early structural studies on the aspartic proteinases realized that the two domains were conformationally homologous and were related by a twofold axis that passes through the center of the active site. They are probably the result of an internal gene duplication.[24,25] The active site of the enzyme lies in a long cleft between these two domains and can be located in this figure by the presence of the classic aspartic proteinase inhibitor, pepstatin, whose coordinates have been taken from the crystal structure of its complex with rhizopuspepsin.[26] Each domain contributes an aspartate side chain, residues 32 and 215*, to the active site; each aspartate comes from the homologous position in the respective domain.

The mechanism of activity of the aspartic proteinases is not entirely understood, despite many years of effort. The active site is composed of the two aspartate residues mentioned above, 32 and 215. At the pH optimum of most aspartic proteinases, around 2, at least one or both of these aspartates are protonated. There is also a water molecule bound between the aspartates,[27] and it is hydrogen bonded to them (see Figure 4a). The putative transition state (Figure 4b) has a water added to the carbonyl of the scissile bond to form a tetrahedral intermediate. Presumably, renin has a similar transition state, despite its much higher pH optimum of around 6.5.[28] The discovery of pepstatin[13] with its unusual statine residue indicated that a hydroxyl at the position of the carbonyl could serve as a transition-state analog or, as some call it, a combined substrate analog[29] (Figure 5a). Statine has two extra atoms in the main chain, making it quite different from a standard residue. Norstatine would serve as a similar transition-state analog and would have only one extra atom in its main chain (Figure 5b). The hydroxyethylene isostere is another replacement, with the additional advantage that it is isosteric to a peptide bond (Figure 5c). Less obvious and less potent, although synthetically easier to prepare, is the reduced amide (Figure 5d), which can substitute for the peptide bond at the scissile position, even though it has a charged nitrogen.

As can be seen in Figure 2, there are a number of critical stretches of chain that surround the active site — the region of greatest interest to us in understanding the catalytic and substrate/inhibitor binding properties of renin, and in drug design. The portions of the protein that include the two aspartate residues are very highly conserved in both their sequence and three-dimensional structure. Thus, it is likely that any member of the aspartic proteinase family will share this conformation. However, there are several loops that delimit the substrate/inhibitor binding site that require special attention in the modeling process. These loops include the "flap" — a range of residues around the highly conserved Tyr 75. The residues of the flap form intimate interactions with a bound ligand. Figure 2 shows that the three fungal crystal structures have quite different conformations around residues 75 to 80. The sequence alignment (Figure 3) suggests that the number of residues in this flap will be different in renin than in the fungal proteinases, which would require the renin molecule to have a different conformation for this loop. The other major loop problem in the immediate active site area includes residues 290 through 300. In both renin and pepsin there is a four- to five-residue insert that is not present in any of the fungal enzymes or in bovine chymosin (see Figure 3). In addition to the insert, this loop has a rather strange composition in renin, with a consecutive Pro-Pro-Pro sequence. The interaction of this larger loop in renin with the substrate/inhibitor may be expected to be quite different than in the fungal enzymes. We will be examining the various model structures to see how they model these loops and their detailed interactions with substrate or inhibitors.

The models of renin can be used to examine the mode of binding of substrates or inhibitors. Experimental structures exist for complexes of

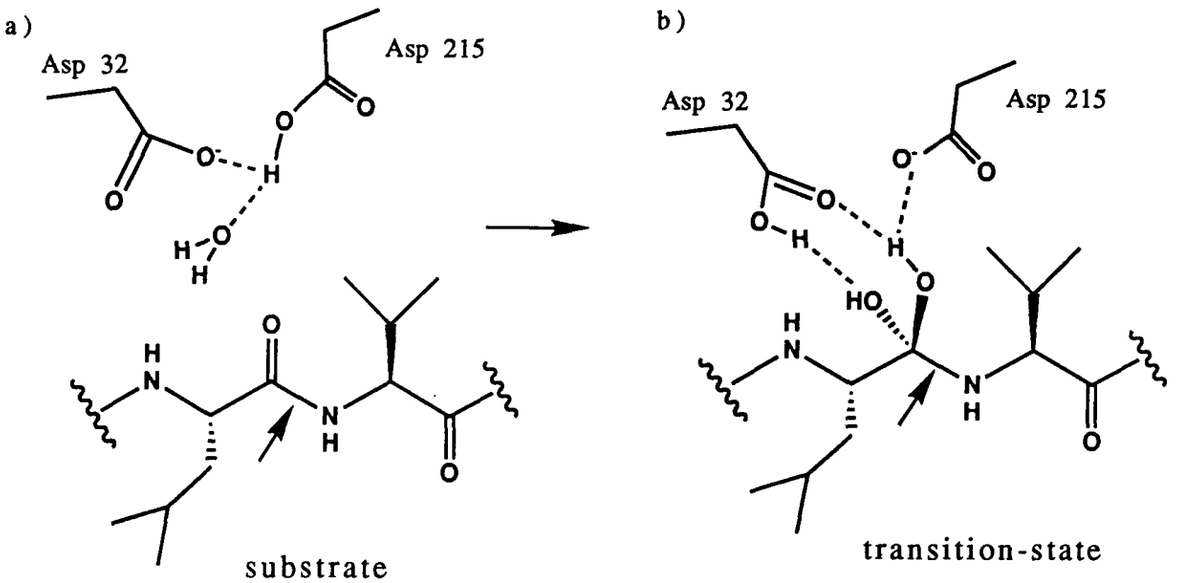

FIGURE 4. (a) Schematic diagram of the aspartic acids in the active site of the aspartic proteinases with a water molecule bound between them. The arrow marks the bond to be cleaved. (b) Proposed tetrahedral transition state of amide bond hydrolysis.

several fungal enzymes with pepstatin[26,30] and for some of these proteins with renin inhibitors.[31-34] The various models predict binding conformations for the substrate/inhibitor on the enzyme. The models will be examined to see how they bind the respective residues of the substrate or inhibitor in the area of the active site. We will be looking at these binding subsites for the source of the very high specificity of renin for angiotensinogen — its only known substrate. The detailed structures of these subsites will also be critical for designing highly potent, novel inhibitors of renin.

The functional properties of renin are of great interest. While an acknowledged member of the aspartic proteinase family, renin differs from the other members of the family by having a pH optimum around 6.5, rather than the low value of 2.0 that is characteristic of pepsin.[28] Thus, an important question that has been asked is whether the models provide any indication as to the molecular basis for this remarkably high pH optimum of renin.

B. The Published Model Structures of Renin

The models that have been reported in the literature will be described in this section. It is useful to include a few introductory comments to help focus the basis for comparison. The only coordinates that are available to us are those for our own models.[35-37] Therefore, a direct detailed comparison of the structures is not presented in this review. Many of the figures that appear in these papers are difficult to decipher in the detail needed to perform a meaningful comparison. Therefore, we attempt to use whatever information is presented in the papers to highlight the similarities and differences, if any, between models.

Because of the nature of the comparative modeling method, all the model structures will resemble each other to a considerable extent. This is because they are derived from one or more of the known aspartic proteinase structures, which are themselves very similar (Figure 2). Thus, virtually all the models share certain common properties. We will summarize them here to avoid having to repeat them in the description of each of the models. The putative glycosylation sites on renin, residues Asn -2 and Asn 67, lie on the surface of the molecule, as expected, where they are accessible to the glycosylating enzymes of the cell. Mouse renin is cleaved into two noncovalently associating fragments *in vivo*. The

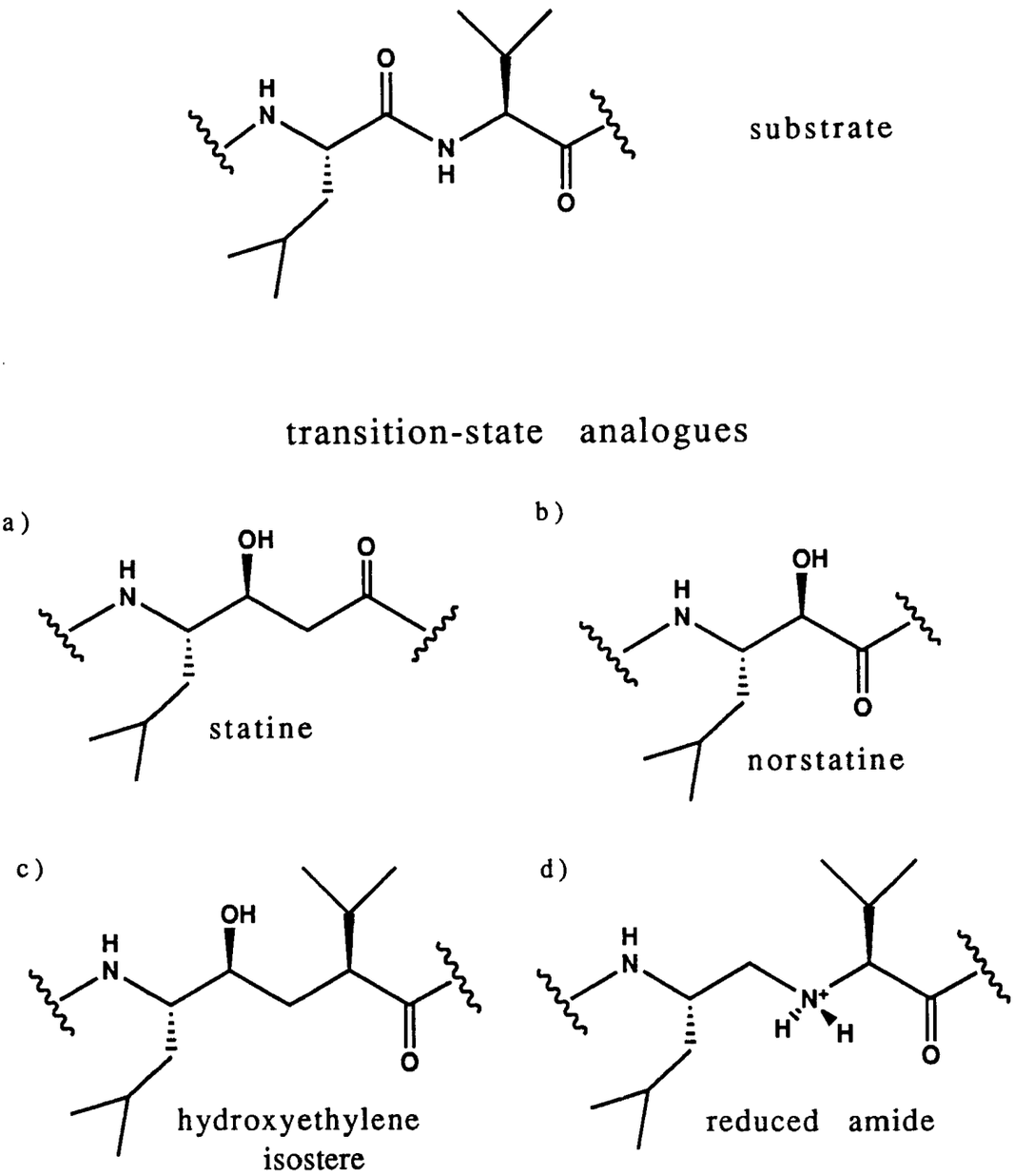

FIGURE 5. Structures for a variety of common transition-state analogs.

cleavage site lies in the loop between residues 280 and 285. The models all show that this loop is external and is highly exposed. Unless otherwise noted, all possible disulfide bridges that are homologous to ones in the other aspartic proteinases are formed. Finally, the model structures show that the appropriate exon/intron boundaries[19] all lie on the surface of the molecule accessible to solvent, as predicted.[38]

The comparative modeling method depends critically upon the initial alignment of the sequence of an unknown protein (renin) to the sequences of the known structures (the aspartic proteinases).[6,9] Differences in the alignment may cause particular residues of the sequence to be placed at different positions in the three-dimensional structure. When this difference in alignment occurs in the variable external loop regions

of the molecule, since these regions, in any case, may have a different conformation from any of the known structures, the difference in alignment may not be significant. However, when it occurs in a structurally conserved region of the known aspartic proteinase structures, then the difference in alignment will result in a very different model structure at this point in the molecule. Such cases, when they occur, will be presented in the following discussion; the significant differences in alignment between the models are summarized in Figure 6.

Several of the groups have modeled both the mouse submaxillary gland renin and human renal renin. Because of the main interest in the human structure for drug design purposes, we will concentrate here on the human model structures only.

All of the groups used the experimentally available inhibitor-proteinase complex structures to model the binding of inhibitors to the active site. The information available when most of the initial modeling was performed was of a pepstatin fragment bound to penicillopepsin[30] and of pepstatin bound to rhizopuspepsin.[26] The nature of the structure of pepstatin is such that the P_4* through P_1 positions correspond to normal amino acids and can be used directly to model peptide inhibitors. However, the unnatural amino acid statine has an unusual main chain that does not permit its use as a direct analogy to normal peptide inhibitors (Figure 5a). The initial hypothesis was that the first statine of pepstatin would mimic only the P_1 residue, with the hydroxyl group of statine acting as an analog of the transition state of amide bond hydrolysis. However, accommodation of the extra atoms of statine, without forcing all the subsequent residues out of their normal binding sites, then became a major problem. Examination of the X-ray structure of pepstatin in rhizopuspepsin[26] with a model octapeptide substrate superimposed, indicated the statine may act as a dipeptide analog.[39,41] Fitting the backbone conformation of the peptide substrate onto the backbone of pepstatin in the X-ray complex gave a conformation of the natural substrate where statine was taking the place of both the P_1 and P_1' residues (Figure 7). The Ala of pepstatin approximately coincided with the P_2' position of the substrate, both in main-chain as well as side-chain interactions. The substrate conformation was energetically acceptable and did not have bad steric interactions with the active site of rhizopuspepsin. The side chains of the substrate could also fit into the appropriate binding sites. Powers[42] also concluded statine acted as a dipeptide replacement in statine-based inhibitors of pepsin. The conclusion that statine acted as a P_1-P_1' dipeptide transition-state analog was very important for the understanding of enzyme-substrate interactions and for the further design of statine-based renin inhibitors.

Several of the models and enzyme-inhibitor complexes were refined using energy minimization and molecular dynamics methods. A review of these methods may be found in Burt et al.[43]

1. Blundell/Pfizer and Co-Workers

Blundell and co-workers were the first to report a three-dimensional model structure for mouse submaxillary gland renin[44] and for human renal renin.[45] The structures were modeled primarily from the native fungal aspartic proteinase endothiapepsin.[46] The modeling was performed using the program FRODO.[47] Additions and deletions were modeled with FRODO from other known structures. The model was then optimized by hand on the interactive graphics system. Attempts at energy minimization led to unacceptable movements of the water molecules in the active site and were abandoned. The paper does not describe the source of the water molecules that were included in the renin structure.

The renin substrate was docked as follows. Sites P_4-P_1 were placed according to the corre-

* The residue numbering system used throughout this review refers to the residue numbering of pepsin. These numbers are used for all the other enzymes, as well, in order to simplify comparison of the structures and the sequences. The correspondence between the pepsin numbering and the sequences of all these proteins is given in Figure 3. The nomenclature used for the substrate and inhibitors is that of Schechter and Berger,[112] which describes the residues N-terminal to the scissile bond as P_1, P_2, P_3, . . . , with the numbers increasing as the residues are farther from the scissile bond. The residues C-terminal to the scissile bond are called P_1', P_2', P_3', . . . The numbers also increase as the residue is farther from the scissile bond.

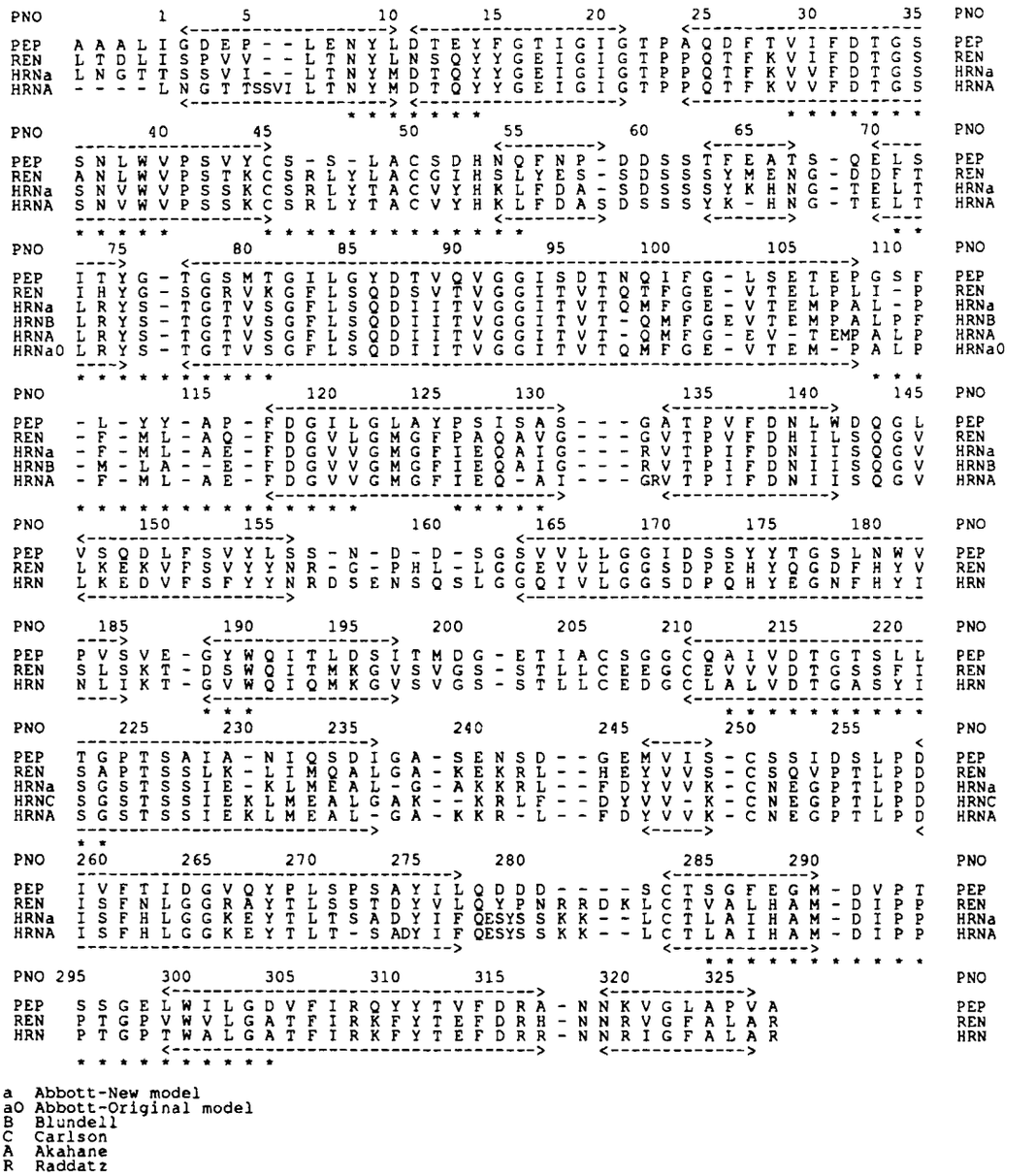

FIGURE 6. Differences in alignment between the various model structures in the structurally conserved regions. Differences in alignment in the variable regions have been largely ignored (see text).

sponding residues in the pepstatin complexes with aspartic proteinases.[26,30] P_1' to P_3' were fitted in the remaining half of the active-site cleft, placing P_1' close to residues 213 and 301 and P_3' near 189. The contacts formed by the inhibitor residues in this model are summarized in Table 3.

One significant difference between this structure and the other models involves the region around residue 102, where in order to align a Phe-Gly sequence of renin to a similar sequence in pepsin, these authors introduce an addition and a deletion relative to the pepsin sequence in the middle of a structurally conserved region of the molecule (Figure 6). As a result, their structure in this area will be different from any of the other models. This region of the molecule is adjacent

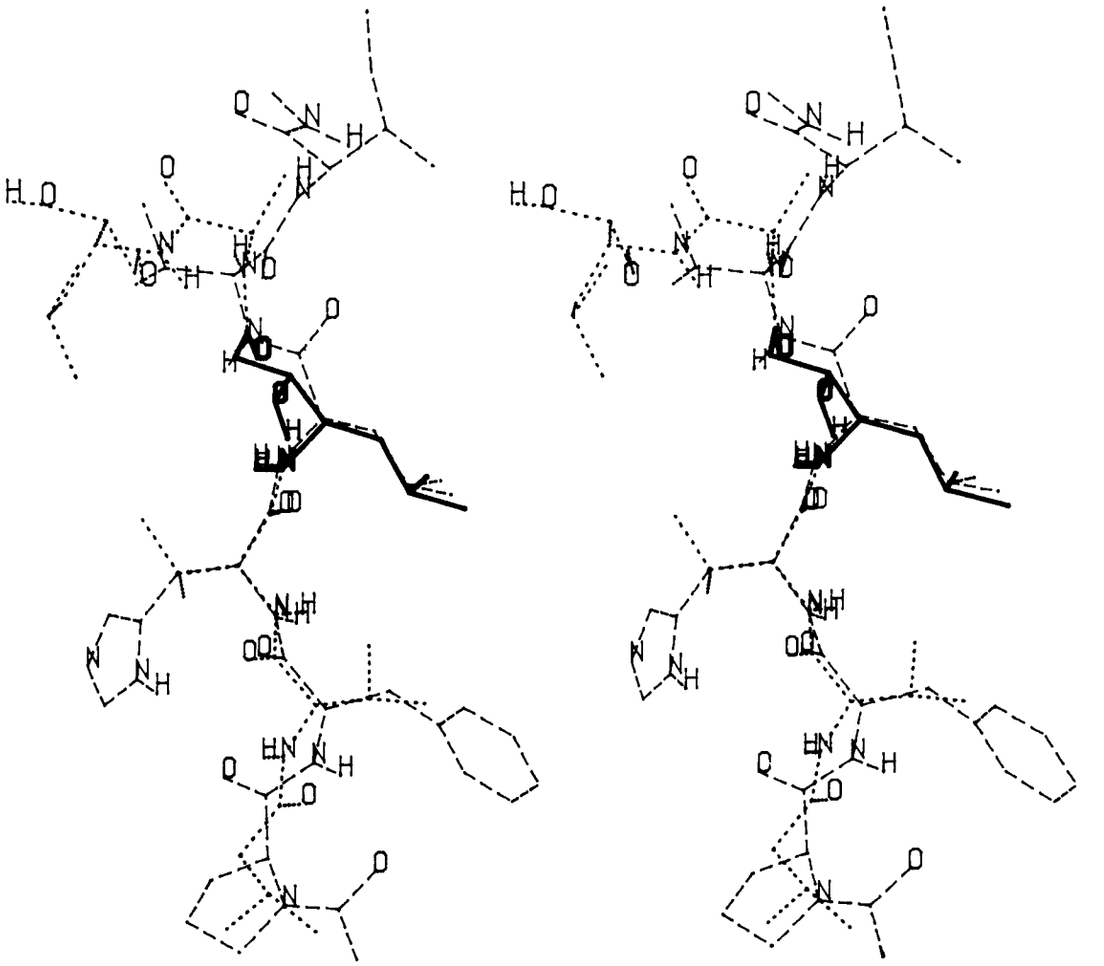

FIGURE 7. Overlap of pepstatin (dotted) with a portion of the natural substrate (dashed). The first statine of pepstatin (solid) spans both the P_1 and P_1' residues of the substrate.

```
PNO        135          140
           <------------------------>

PEP        G A T P V F D N L W
HRNa       R V T P I F D N I I
HRNB       R V T P I F D N I I
HRNB'      T P I F D N I I S Q

           <------------------------>

PNO'       135          140
```

(Scheme 1)

HRNB: taken from Sibanda et al.[45] (Figure 6).
HRNB': actual model in Sibanda et al.[45]

to the inhibitor binding site at P_3 and thus will have a significant influence on our understanding of the P_3 binding subsite.

Another major difference appears at residues 133 to 141. Close examination of the structure figures in the paper by Sibanda et al.,[45] shows that, despite the alignment cited in the paper for this region and shown in Figure 6, in fact, the structure is modeled with a different alignment (scheme 1).

As a result, Asp 138, which is conserved in all aspartic proteinases (see Figure 3), is placed in the position of Ile 140 and is buried in a hydro-

TABLE 3
Nearest Neighbors of the Various Binding Subsites

Subsite	Blundell[a]	Akahane[b]	Carlson[c]	Abbott-original[d]	Abbott-new[e]
S_4	**Y220**, T284, M10, D245, S219, Y275	T77, Y220, D245, T284, H288, M290	**T77, S219, F244, Y246, Q279**	**S219, Y220**	**S219, Y220, H287**
S_3	**T12, Q13, F111,** S219, P110, A114	Q13, W39, L71, L73, Y75, T77, G78, V80, V104, M107a, L110, P111, L114, F117	**T12, Q13, T77, L114, E116, F117, G217, A218, S219, Y220**	**Q13, T77, P110, E116, F117, S21**	**T12, Q13,T77, F112, L114, A115, F117, G217, A218, S219**
S_2	**T77, S76, A218,** H288, Y220	Y220, S222, I228, I287, H288, M290	**S76, T77, G78, D215, G217, A218, S219, Y220, S222**	**T77, G217, A218, S219, Y220, S222**	**S76, T77, G217, A218, Y220, S222, H287, M289, A300**
S_1	**Y75, T77, V120, V30, F111, D32,** W39	V30, G34, S35, N37, W39, L71, L73, Y75, V120, G217	**V30, D32, G34, S35, Y75, T77, V120, D215, G217, A218**	**Q13, D32, Y75, S76, T77, G78, F117, V120**	**V30, D32, G34, S35, W39, Y75, T77, G78, F112, F117, V120, D215, G217, A218**
S_1'	**L213, D215,** A301, S222, T216, T299, V189	L213, D215, A301	**D32, G34, R74, Y75, S76, T77, D215**	**G34, S35, S76, L213, D215, G297, P298**	**G34, S35, Y75, S76, V189, L213, D215, I291, P292, A300**
S_2'	**S35, L73, Q128, R74**	I192, Q193, M194, P293, L211, L213	**G34, S35, N37, L73, R74, Y75, S76, Q128**	**G34, S35, S36, N37, L73, R74, Y75**	**G34, S35, S36, N37, L73, R74, Y75, I130, P292**
S_3'	**T187, V189, Q191, L213, Q128**	—	**L73, R74, Q128, A129, I130**	**R74, Y75**	**Q128, I130, V189, L213, I291, P292, P294, T295**

[a] Neighbors of the angiotensinogen sequence. Bold residues <4.5 Å from substrate, others are >4.5 Å.
[b] Neighbors of Boc-Phe-His-Sta-Leu-(4-amido-1-benzylpiperidine). No distance criterion given for choice of neighbors.
[c] Neighbors of the angiotensinogen sequence. Bold residues within 4.5 Å from substrate. (From W. D. Carlson, personal communication.)
[d] Neighbors of the angiotensinogen sequence. Bold residues <4.5 Å from substrate.
[e] Neighbors of Pro-Phe-His-Cha(CHOH-CH_2)Val-Ile-His. Bold residues <4.5 Å from inhibitor.

phobic pocket in the actual Blundell structure, which could be energetically very unstable. The Ile labeled as position 136 is found in the position where this Asp should be and is pointing out into solvent (see Figure 2 of Sibanda et al.[45]). As a result, this portion of the Blundell molecule, which is adjacent to but not in the immediate inhibitor binding site, appears to differ significantly from all of the other models.

These authors were the first modeling group to point out that residue 304, which is an Asp in all the other aspartic proteinases (Figure 3), is changed to an Ala in both mouse and human renin, leading to the speculation that the absence

of this normally conserved negatively charged residue may be the basis for the unusually high pH optimum of renin relative to the other aspartic proteinases. Human renin (but not mouse) also has the unique change of the highly conserved Thr 218 to an Ala. The hydroxyl of the Thr (or Ser in mouse renin) forms a hydrogen bond to one of the carboxylate oxygens of the Asp 215 in the known aspartic proteinase structures. This hydrogen bond is missing in human renin only, so it cannot account for the high pH optimum.

In this model, the unusual Pro-Pro-Pro loop is not directly involved in the substrate/inhibitor binding but is pictured as near the surface region of the protein adjacent to the binding cleft. Nothing is said of the modeling of the difficult flap loop, residues 75 to 80, which must be in intimate contact with the substrate/inhibitor. The flap in renin has a different number of residues than the same loop in endothiapepsin, so it must have been modified significantly during the modeling. The figures in the article show that the flap forms a β-turn at residues 75 to 78, but do not show what detailed interactions are made with the substrate/inhibitor.

In a preliminary report of model structure refinement, Blundell[31] carried out energy minimization studies of the endothiapepsin-H-142 complex and native endothiapepsin *in vacuo* and with the crystal waters.

Pro-His-Pro-Phe-His-Leu^{R}Val-Ile-His-Lys
H-142

The positions of the 345 waters in the endothiapepsin calculation were taken from the crystal structure, and the orientation was initially determined by a rotational grid search for each water. The structures were minimized initially with restraints on all heavy atoms, then the restraints were gradually reduced during further minimization steps, followed by unrestrained conjugate gradient energy minimization. The renin model was also minimized without waters. The calculations were carried out using the AMBER[48] forcefield on a Cray-1S. The energy minimization clearly relieved the bad steric contacts in all the structures. The inclusion of crystal waters in the calculation better preserved the crystal hydrogen-bonding patterns by preventing collapse of hydrophilic side chains onto the surface of the enzyme. Some regions, especially the exposed loops, moved during the minimization, since the hydrogen bonding groups on the surface attempted to form hydrogen bonds. Strain may have been introduced in the initial structure during the model construction process that was relieved by changes in the conformation during the minimization. The flap residues, which could not be precisely determined in the endothiapepsin X-ray structure, although the general conformation was reasonably well defined, moved significantly during the minimization for both of the above reasons.

2. Carlson and Co-Workers

The human renin structure has also been modeled by Carlson and co-workers.[49,50] The renin sequence was aligned to that of pepsin and of the three fungal aspartic proteinases. The renin structure was then modeled after the crystal structure of the fungal enzyme from *Rhizopus*.[51] Rhizopuspepsin was used because in their alignment it showed the highest sequence homology to renin (30 vs. 20 to 21% for the other fungal enzymes) among the fungal proteinases whose crystal structures were known at that time (Figure 3 and Table 2). Unfortunately, this homology assessment for the rhizopus enzyme was based upon a tentative sequence assignment derived from the crystal structure. Such sequences are known to be highly inaccurate and show abnormally high homology, because in cases of ambiguity the homologous sequence is favored. Later determination of the actual rhizopuspepsin sequence[52] shows that it is not significantly more homologous to human renin than are the other fungal enzymes (Table 4). Additions and deletions relative to the rhizopuspepsin structure were introduced by manual manipulation on an interactive graphics system. No details were given as to how the critical loops in the immediate active-site area, including the variable flap and the addition at the Pro-Pro-Pro loop, were modeled. The model structure was refined using the molecular mechanics energy program CHARMM.[53] The protein structure was subjected to 400 cycles of energy minimization, enough to remove bad contacts and correct bad

TABLE 4
Percent Sequence Identity for the Aspartic Proteinases

	Mammalian		Fungals			Renins	
	PEP	**CHY**	**PEN**	**RHI**	**END**	**REN**	**HRN**
PEP	*1.00*	0.58	0.31	0.37	0.27	0.42	**0.38**
CHY		*1.00*	0.28	0.32	0.24	0.36	**0.36**
PEN			*1.00*	0.39	0.51	0.25	**0.22**
RHI				*1.00*	0.35	0.26	**0.24**
END					*1.00*	0.23	**0.23**
REN						*1.00*	**0.68**
HRN							*1.00*
Total	330	325	323	325	330	336	338

geometry, but not long enough to achieve a true minimum-energy structure.

Pepstatin and two hexapeptide substrates were modeled into the active site based upon the crystal complex structures of pepstatin and the pepstatin fragment bound to the fungal enzymes.[26,30] The residues forming the respective binding subsites for a peptide substrate are listed in Table 3. The authors found that the side chain of the second statine in pepstatin at position P_3' of the inhibitor bound in the same hydrophobic pocket as the P_1' side chain of the peptide inhibitors. This is a quite different position from the P_3' subsites found in the other models. The authors also noted that the positions of the Leu side chains of the P_1 and P_1' sites were somewhat different in the peptide vs. the statine inhibitors. They could not reach as far into the respective hydrophobic subsites as could the statine side chains, but had to be moved toward the center of the active site.[49] The active-site residues were found to be almost identical to the other aspartic proteinases, with the exception of the unique change in human renin of Thr 218 to Ala. This change would remove a conserved hydrogen bond to Asp 215 and thus could change the electrostatic potential considerably at the active site.

The authors attempted to explain differences in the specificity, especially at the P_1' site, between human renin and mouse renin, which they also modeled.[54] Mouse renin does not cleave human angiotensinogen, however, human renin will cleave both primate and nonprimate substrates. The differences were ascribed to a change of Leu 213 in human to Val 213 in the mouse sequence, allowing mouse renin to accommodate the larger Leu P_1' side chain of nonprimate renin substrates rather than the Val P_1' residue that occurs at this site in human angiotensinogen. The fact that human renin cleaves both primate and nonprimate angiotensinogen means that it must be able to accommodate both the Val and the Leu side chains at P_1', despite the larger residue, Leu 213, of human renin partially filling the pocket. This fact was explained by a conformational change causing a change in the shape of the P_1' pocket of human renin that was not described in any significant detail in the papers.[49,50] The importance of sequence changes between human and mouse renins on the flap (residues 68 to 78) was difficult to assess, because the sequence differences were found to lie on the solvent-accessible surface, rather than facing the rest of the protein or the substrate/inhibitor.

3. Akahane/Kissel

Another model reported for human renin represents a *tour de force*, as it was constructed using physical models rather than on a molecular graphics system.[55] The structure was based on the fungal enzyme, penicillopepsin.[56] This model structure was the only one of all the reported renin structures that left two of the cysteine residues unbridged, positions 206 and 210, in response to the early report of Misono and Inagami[57] that there was at least one free cysteine in human renin. While this is a significant departure from any of the other models, its importance is mitigated by the fact that these residues are relatively distant from the active site. Additions and dele-

tions were duly constructed, with special attention being given to the large addition at the Pro-Pro-Pro loop. Some of the additions and deletions were reported to be compensatory in the structure.

These authors also noted the important change of Thr 218 to Ala in human renin (only), thereby losing a hydrogen bond to the active-site Asp 215. Also described, as Blundell and co-workers had reported earlier,[45] was that the conserved Asp 304 in all other aspartic proteinases becomes Ala in both human and mouse renin.

Several inhibitors were constructed into the renin structure, including two statine-based analogs and a N-terminal peptide ending with leucinal at the P_1 site. The inhibitors were built into the model based upon the crystal complex structures of a pepstatin fragment on penicillopepsin.[30] The renin residues occupying the respective subsites are given in Table 3. These authors discussed some of the structure-activity data available for renin inhibitors. Thus, the importance of a possible hydrogen bond between the side chains of His P_2 and Ser 222 was tempered by the observation that Phe is an acceptable replacement at the P_2 site. The favorable placement of a large hydrophobic residue at the P_3 site, such as Phe, was explained by the presence of a larger S_3 subsite in renin over penicillopepsin due to a change of Phe to Pro at position 111.

4. Abbott — Original Model

Another model structure for renin was reported as part of a series of studies to design novel renin inhibitors.[35,36,58] Four known crystal structures for aspartic proteinases, the three fungal structures, and a partially refined structure for porcine pepsin[59] were used (Table 1). Paradoxically, while the pepsin structure was clearly the most homologous to renin (Table 4), it was also the least well-refined crystal structure. The model was constructed largely from the pepsin coordinates because of the higher homology; however, the highly conserved active-site region was taken from the more highly refined fungal enzyme structures. Special efforts were taken to model the critical loops in the structure in the immediate region about the active site. These included the flap, which was taken from the homologous pepsin loop. The Pro-Pro-Pro loop has the same length in pepsin as in renin; however, the conformation that this loop adopted in the pepsin structure would not accommodate a Pro-Pro-Pro sequence. Instead, this loop was built from the observed conformations of Pro-Pro-Pro sequences found in the known structures of other proteins in the Brookhaven Protein Data Bank.[60]

The hexapeptide inhibitor corresponding to the angiotensinogen sequence and having a reduced amide at the scissile bond was placed in the active site on the structure of pepstatin bound to rhizopuspepsin.[26] The P_3 through P_1 residues could be modeled directly from pepstatin. However, the C-terminal portion of the hexapeptide inhibitor could not follow the conformation of pepstatin because of the unusual main chain of the statine residue. It was modeled by systematically rotating each of the main-chain torsion angles in pairs, starting with P_1' through P_3', and determining the possible docking sites for the side chains of the inhibitor on the enzyme. Clear and unambiguous subsite pockets were found for the Val P_1' and Ile P_2' residues. However, several possible positions could be identified for the side chain and C-terminus of His P_3'. The structure was refined by energy minimization using the molecular mechanics program VFFPRG.[61] Just the immediate active-site environment, including all residues within 7 Å of any atom in the inhibitor, was minimized, as previously described.[36,58] The reason for limiting the energy refinement to the environs of the active site was that the increasingly poorer agreement of the known structures as one moved away from the active site made the more remote portions of the renin model much less reliable and therefore not worth further refinement. Residues comprising the inhibitor binding subsites of this model are given in Table 3.

5. Raddatz/E. Merck

A group at Merck in Germany started with the published crystal structure of penicillopepsin and developed a model of renin.[62] The backbone conformation was kept constant and the amino acid side chains mutated to the human renin sequence. The side chains were oriented to mini-

mize steric overlap with the other residues. The authors do not mention their sequence alignment or how the insertions and deletions were done. This renin model was then compared with the Blundell renin model, and it appeared that the Blundell model accounted better for the interactions between the enzyme and the inhibitor, especially for the flap residues. Therefore, the flap region of the Blundell model was adopted for use in the Raddatz model.

An octapeptide substrate was built into the active site using the conformation of other inhibitor/protease structures. The energy of the enzyme-inhibitor complex was then minimized with the program CPECM (Conformational Potential Energy Calculations for Macromolecules).[63] Other inhibitors (H-142, SCRIP, and pepstatin) were also built in the renin model and the energy was minimized. The resulting conformations of the inhibitors were found to be similar to that of the substrate.

6. Abbott-New, A New Renin Model

Recently, we initiated a new modeling effort on the human renin molecule[37] because of the availability of significant, new structural information on the mammalian aspartic proteinases (Table 2). A highly refined structure of porcine pepsin was produced by Abad-Zapatero et al.[64] at Abbott. In addition, Gilliland and co-workers[65] have generated a refined high-resolution structure for the closely homologous bovine chymosin (Table 4). For the first time, then, two highly refined mammalian proteinase structures are available, which should permit more accurate extrapolation to a model renin structure.

Figure 8 shows a comparison of the pepsin and chymosin structures. It can be seen that the two structures are highly conserved in their conformations. This comparison, together with the high homology of the two proteins to renin (Table 4), gives us increased confidence that the mammalian enzymes are closely related and that extrapolation to the renin structure is more likely to be accurate. The sequences of pepsin and chymosin, as well as those of the fungal enzymes, were aligned based upon the three-dimensional structure overlap (Figure 3).[6,9] We then aligned the human and mouse renin sequences to those of the known structures. Based upon this alignment, a new model of renin was constructed using methods that have been described.[6,9]

A hexapeptide inhibitor was modeled into the active site based on the rhizopuspepsin-pepstatin inhibitor complex crystal structure conformation.[26] The energy of the resulting structure was then minimized using DISCOVER.[66] All atoms were tethered to their initial positions. The restraining force was decreased in steps over 2000 minimization cycles. Nearly 300 water molecules were added to prevent large movements of loops and side chains. The majority of these were in the active-site region. The model was then further refined with another 500 cycles of minimization. The RMS deviation between the old and new Abbott models is 3.3 Å. The major factor in the difference between the models is due to the RMS difference between the old[59] and new[64] pepsin crystal structures. The overall RMS deviation between the Cα coordinates of the two pepsin structures is 3.0 Å. Despite this large RMS deviation, the N-terminal domain, and especially the active-site regions, are very similar between the two Abbott models (Table 3). The Cα coordinates of the active sites have an RMS difference of 0.7 Å, primarily because the original Abbott model took the immediate active-site coordinates from the better refined fungal proteinases (as noted above). Since the new Abbott model is based on the more refined pepsin structure, the renin model has significantly better geometry and does not change significantly during energy minimization and molecular dynamics.

C. The Crystal Structure of Human Renin

The recent publication of the experimental structure for human renin prepared from recombinant sources[12] allows us to consider an approximate comparison with the model structures. A full, detailed comparison is not possible at this time, since the experimental coordinates are not yet available.

Figure 8 shows a Cα plot of the experimental renin coordinates taken from the publication, together with the experimental structures for pepsin

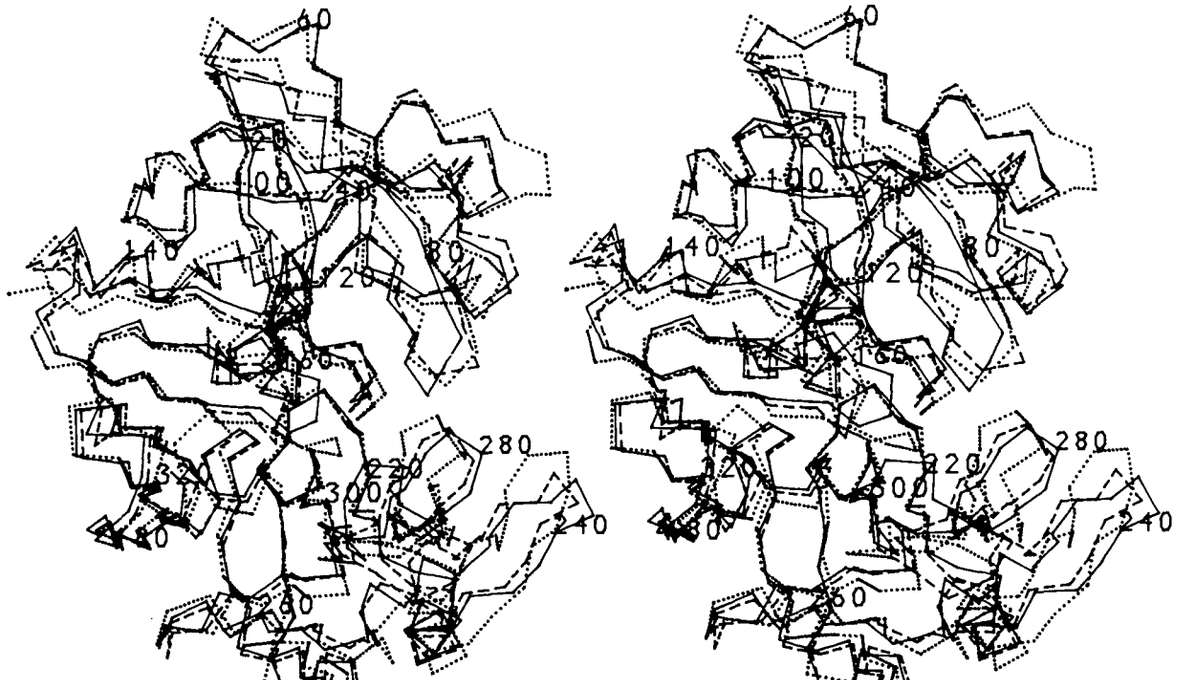

FIGURE 8. Overlap of the refined pepsin (3PEP, solid) and chymosin (1CMS, dashed) structures with the coordinates developed for the recently reported experimental structure (dotted) of renin.[12]

and chymosin. It is clear that, qualitatively, renin is as closely related to pepsin and chymosin as they are to each other, corroborating and validating the use of these two proteins to model the renin molecule using the comparative methodology. The major differences appear at the external variable loops, exactly as expected.

A more interesting comparison involves our recent model of renin, described above, and the reported experimental renin structure shown in Figure 9. The conserved regions agree quite well, as expected from the agreement of the known structures shown in Figure 8. The major differences include several variable regions of the molecule on the external surface. In particular, these are the loops around residues 235 and 275, which lie adjacent to the active site and may interact with residues P_4 and P_5 of the substrate/inhibitor. As to the immediate loops around the active site, the flap (residues 75 to 80) is very similar in the model and the experimental structures. Deviating much more dramatically is the conformation of the Pro-Pro-Pro loop (resides 290 to 300). In the model structure, this loop lies at the edge of the active site, where it would make intimate contact with the bound substrate or inhibitor, a conformation taken from the pepsin structure (Figure 8). The crystal structure of renin shows that this loop is pulled 5 to 6 Å away from the active site into the C-terminal domain and would not be expected to interact at all with ligands bound to the active site. Of course, the experimental structure of renin is that of the native enzyme and not of an inhibitor-bound complex. A complete and more definitive comparison must await the availability of coordinates for renin and, especially, for a renin-renin inhibitor complex structure.

III. APPLICATION OF RENIN MODELS

The renin models have been used for a variety of applications. The model structures of renin have been used to guide selection of peptides for use as haptens in antibody production. These antibodies could be useful tools for biochemical and

FIGURE 9. Superposition of the recently constructed model (solid) of renin[37] on the experimental crystal structure (dotted) of renin.[12] The structures agree quite well, with the exception of the conformation at several of the external loops. In particular, these include the loops adjacent to the active site, such as around residues to 240 and 270. It also includes the immediate active site Pro-Pro-Pro loop, residues 290 to 300, which is significantly different in the model and the experimental structures (see text).

physiological studies of renin and, perhaps, as antihypertensive agents. Conformational features of renin have also been examined through the use of antibody binding studies. These models have also been employed to help understand the mechanism of renin enzymatic activity.

The major use for accurate three-dimensional models of renin has been to understand the structure-activity relationships of renin inhibitors and to design novel inhibitors. In general, the activity studied is *in vitro* renin inhibition, which is clearly related to the structure of the enzyme-inhibitor complex. *In vivo* activity, which depends not only on inhibitory potency but also on bioavailability, metabolic stability, pharmacokinetics, and pharmacodynamics, and is also more difficult and time consuming, has not been considered from a modeling perspective. Interestingly, highly potent *in vitro* renin inhibitors were achieved prior to any of the renin modeling.[67,68] If so, what role then could modeling play in the further evolution of inhibitors? The answer is that the early potent compounds were hexa- or octapeptides and, therefore, metabolically unstable and orally unavailable. The challenge, then, to the modeling was to participate in the design of less peptidic, more stable, and ultimately orally bioavailable analogs that retained high inhibitory potency.

A number of research programs at academic institutions have been interested in aspartic proteases and their inhibitors. Many pharmaceutical companies have had renin inhibitor programs for the development of antihypertensive drugs and have published some of their modeling results. These papers generally describe the modeling of a few inhibitors in a renin model. The steric contacts and conformational energy of the inhibitor may be minimized using a molecular mechanics program, and sometimes, molecular dynamics simulations of a portion of renin with the inhibitor

may be carried out. These relatively large calculations require good model structures and fast computers. The behavior of the inhibitors and the interactions between renin and the inhibitors have been used to explain the differences in *in vitro* activity between compounds and to guide the synthesis of additional inhibitors.

This review will cover only the literature where renin models were mentioned as having played a role in the design or analysis of renin inhibitors and their activity.

A. Antibodies

The renin models have been used to suggest regions of the enzyme that may serve as antibody binding sites in order to develop antibodies that could inhibit the enzymatic activity of renin. The antibody binding studies have also been used to provide experimental support for conformational details of portions of the renin models. Successful preparation of antibodies from short peptides of an enzyme for use in binding of the whole enzyme does not depend on knowledge of the exact three-dimensional structure of the enzyme, but rather on a general idea of whether the particular segment is exposed on the surface of the enzyme. Thus, the renin model structures are ideal for this analysis. However, the conformational details one may expect to glean from a comparison of binding affinities between antibodies prepared against peptides of defined conformation and a protein depends on knowing the exact conformation of the peptide in the peptide-antibody complex. Without crystal structures of these peptide-antibody complexes, our knowledge of the peptide's bound conformation is limited. Also, the recognition sites on the peptide are generally unknown, and these may be only a small portion of the peptide. Consequently, the conclusions that may be drawn from the antibody studies are necessarily limited, but may be useful in certain applications.

Based on the reported good correlation[69] found between the surface accessibility of residues of a protein, when calculated using large probe radii, and antigenicity, Evin[70] calculated the surface accessibility of the residues of the Carlson renin model using a 10 Å probe. The surface area for all atoms of each residue was compared with the surface area of the same residue isolated and in an extended conformation. The percent of the surface area that would be accessible in the renin model structure relative to the surface area of the extended conformation was calculated and used to guide peptide selection. Seventeen peptide segments were predicted to be epitopes. Six of these peptides were prepared and tested against 11 different polyclonal antibodies prepared against human renin. Five of the six peptides were recognized by at least one of the polyclonal antibodies. Peptides *5-2* and *5-3* (Table 5), corresponding to the region near Cys 206 and Cys 210, were recognized by a number of the antibodies and support the existence of a disulfide bond in renin between residues Cys 206 and Cys 210, as in pepsin. This is of interest because, based on the report[57] that there are free cysteines in renin, the Akahane renin model suggests Cys 206 and Cys 210 are free cysteines. Purified antibodies to two of the peptides, *5-1* and *5-2* of Table 5, inhibited cleavage of angiotensinogen but not of the tetradecapeptide substrate representing the N-terminal portion of angiotensinogen. Presumably this is due to the fact that these two peptides are not located in the immediate active-site cleft, although they are close (Figure 10). Antibodies to these peptides may hinder the binding of angiotensinogen, but not the tetradecapeptide substrate. Antibody to peptide *5-4*, with the sequence of the Pro-Pro-Pro loop, inhibited cleavage of both substrates, presumably because binding of the antibody interferes directly with renin-substrate complex formation.

TABLE 5
Peptide Sequences Recognized by Antibodies to Human Renin

	Sequence	Pepsin sequence number
1	YIEQAIGRVTPIF	Y-125-137
2	YLLCEDGCLAL	Y-203-213
3	YGSSTLLCEDGCLAL	Y-199-213
4	YIHAMDIPPPTG	Y-286-297

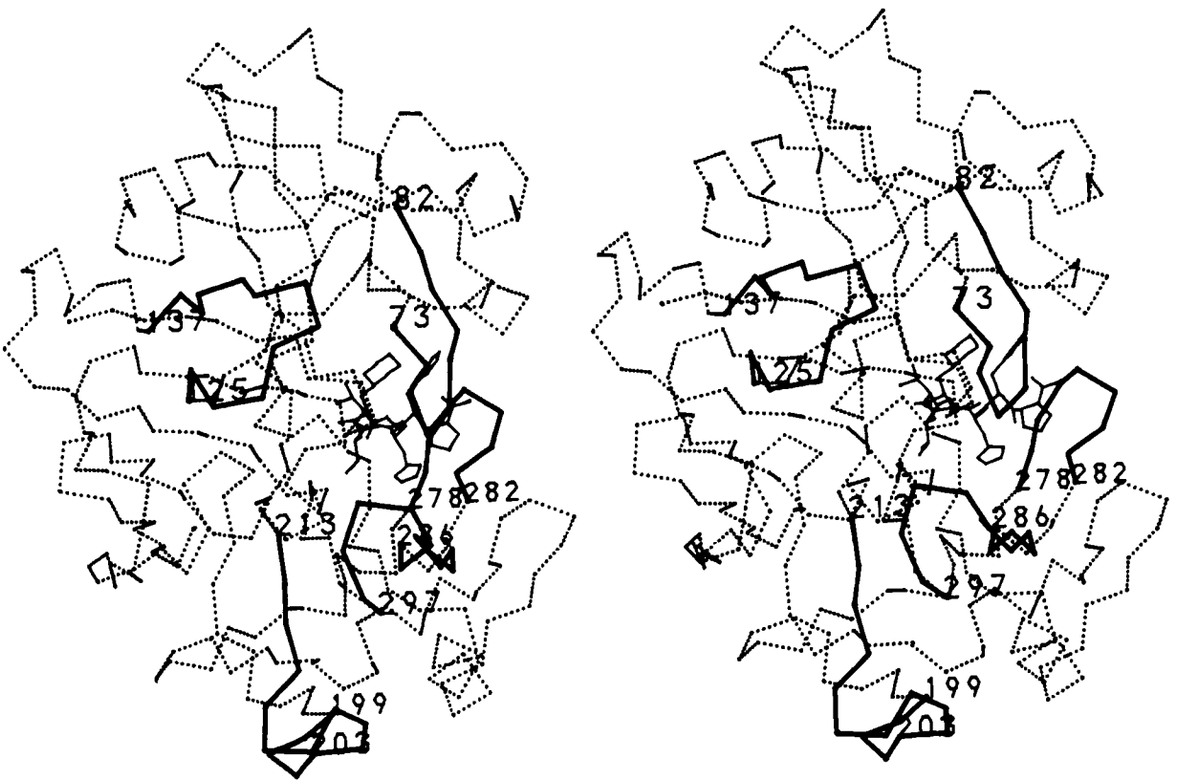

FIGURE 10. Cα plot of the new Abbott renin model (dotted) showing location of peptides (solid) used to prepare antibodies.

Based on a model of mouse submaxillary gland renin by Blundell,[44] Bouhnik et al.[71] prepared seven peptides from segments of renin that were exposed on the surface of the enzyme near the active site and where the sequence was peculiar to human renin (Table 6). Monoclonal antibodies to pure human renin did not recognize any of the peptides. Several of the peptides reacted with polyclonal antibodies to human renin. Antibodies prepared against five of these peptides were able to bind human renin and to lower enzymatic activity. One of the antibodies, made to peptide *6-3* with the sequence of the flap region, was especially antigenic and strongly inhibited enzymatic cleavage of the tetradecapeptide substrate. Examination of the renin model (Figure 10) suggests that binding of an antibody to the flap region would severely interfere with binding of substrate at the active site.

Fehrentz et al.[72,73] prepared peptides with the sequence of the flap region of human renin based on the Blundell model. Two of the peptides, *7-3* and *7-4* (Table 7), were cyclized at the ends by substitution of Cys for the amino acid at the N- and C-termini with subsequent disulfide bond formation. The conformation of each peptide was examined by IR, NMR, and CD spectroscopy. The cyclic peptides were shown to be antiparallel β-strands forming a β-sheet with a β-turn at the

TABLE 6
Renin Peptides Used to Generate Antibodies

	Sequence	Pepsin sequence number
1	Ac-KCSRLYTACVY	44-52
2	YLFDASDSSS-OMe	Y-55-63
3	LRYSTGTVSG	73-82
4	YPFMLAEFDG-NH_2	Y-111-119
5	YNRDSENS-NH_2	155-159
6	GAKKRLFDY-NH_2	237-246
7	QESYSSKKL-NH_2	278-282

Ac = acetyl.

TABLE 7
Sequences of Peptides of the Flap Region Used to Prepare Antibodies

	Sequence	Pepsin sequence number
1	LRYSTGTVSG	73-82
2	TGLTLRYSTGTVSGFLS-NH_2	69-85
3	CLRYSTGTVC-NH_2	C-73-80-C
4	CLTLRYSTGTVSGC-NH_2	C-71-82-C

strand reversal. The linear peptides were much more flexible, since no interstrand nuclear Overhauser effects were observed by NMR. The peptides were tested with polyclonal antibodies to human renin. The linear peptides were not recognized by any of the antibodies, while the cyclic peptides were recognized by all the antibodies, showing that the flap is an important antigenic site. If the conformation of the peptide in solution is similar to the conformation recognized by the antibody, then the conformation of the flap is an antiparallel β-sheet with a β-turn, as suggested by the renin models (Figure 10).

B. Enzyme Mechanism Studies

While the mechanism for peptide hydrolysis by aspartic proteinases is not fully understood, there are a number of features that have been elucidated. The differentially protonated aspartic acids (32 and 215) serve as a general acid and a general base. A water molecule acts as the nucleophile to form the tetrahedral transition state, which collapses to form the products. The pH dependence of renin is unique. Other aspartic proteinases prefer acidic pH, whereas the pH optimum for renin is near physiological pH.

Amino acid differences between renin and other aspartic proteinases have been suggested as the cause of the shift of the pH optimum. Residue 304, which is an Ala in mouse, rat, and human renin, is an aspartic acid in other aspartic proteinases (Figure 3). However, mutation of Ala 304 in human renin to Asp had little effect on the pH dependence.[74] Human renin also has an alanine at position 218, where all other aspartic proteinases have either a threonine or serine (Figure 3). This residue is close to Asp 215 and may influence the pH profile by forming a hydrogen bond to Asp 215. However, both rat and mouse renin have a high pH optimum, even though they have a threonine or serine, respectively, at position 218. The renin models show there are water molecules in the region between the side chains of the P_2 and P_1' residues near Asp 215. A hydrogen bond from one of these water molecules may replace the hydrogen bond from the threonine or serine at 218 in the other proteinases.[75] Therefore these individual residue substitutions do not satisfactorily account for the high pH optimum of renin.

Based upon biochemical and modeling studies,* Green et al.[75] have suggested that the P_2 His of angiotensinogen and other substrates gives rise to the high pH optimum of renin and that, in the presence of this histidine at P_2, renin operates by a different hydrolysis mechanism. Measurement of the pH dependence of renin activity with a tetradecapeptide substrate with His at P_2 showed maximum activity at pH ~7.0. Substrate with a Gln at P_2 gave maximum activity at pH ~5.5. In this mechanism both catalytic aspartic acids are ionized at physiological pH. Modeling suggested that upon binding of the substrate, a hydrogen bond is formed between the protonated His at P_2 and Asp 215 of the enzyme. The effect of this hydrogen bond is to lower the pKa of Asp 215 and to raise the pKa of Asp 32. Asp 32 can then act as a general base to abstract a proton from the bound water molecule, which nucleophilically attacks the scissile peptide bond. In the absence of a histidine residue at the P_2 site, for example, when a glutamine is at P_2, the pH must be lowered to protonate one of the aspartates and then catalysis will proceed by the standard aspartic proteinase mechanism. Additional experiments need to be performed to support this novel mechanism and, in particular, to demonstrate that it explains the dramatic shift in pH optimum of the enzyme from pH 2-3 to 7.

* This study was performed using a model developed at Monsanto by substituting the amino acids of renin into the active site of an endothiapepsin-renin inhibitor complex crystal structure solved at Monsanto and refined using the molecular modeling program PROTEUS. No further details of this model have been presented.

C. Renin Inhibitors

Knowledge of the model structure for renin has had general implications for the design of novel renin inhibitors. As described above, it provides a three-dimensional picture of the active site and the details of the interaction between inhibitors and the enzyme, including hydrogen bonds and hydrophobic interactions. In this section, we review how the models have been used in the design of novel renin inhibitors.

One of the most important consequences of the renin models is that the inhibitor is extended along a groove in the renin structure situated between two domains. In this conformation, the side chains are staggered on opposite sides of the main chain (Figure 11). This implies that there will be little interaction between the different residues in the inhibitor. The consequences of this latter statement for drug design are considerable. What it means is that the problem of designing new inhibitors can be separated into parts, such as the prescissile and postscissile. Each part can be varied and optimized. One can then combine the parts and expect, in general, to get additive (for energy) or multiplicative (for inhibitory constant) effects. Indeed, in most renin-inhibitor structure-activity studies, this expectation is realized to an excellent first approximation, greatly simplifying the drug design process.

Further examination of the inhibitor-renin model complex shows that the specific interactions, such as hydrogen bonds, which are common to all the aspartic proteinase inhibitor complex structures, are primarily between the main chain of the inhibitor and groups on the enzyme (Figure 11). The side-chain interactions of the inhibitor are largely hydrophobic, with the various side chains residing in respective subsites on the enzyme. This suggests that the alignment of the molecule in the active site is due to main-chain interactions, while the specificity of the inhibitor and the binding energy are primarily due to the side chains fitting into their pockets. This implies the general strategy of optimizing the side-chain interactions while preserving the main-chain groups that are involved in specific interactions with the enzyme.

Knowledge of the pattern of the main-chain conformation of the inhibitor and the specific interactions with enzyme groups provides an early advantage in the drug-design process. If it does nothing else, it eliminates from consideration a large number of possible modifications to the basic linear structure of the inhibitor, which would be clearly inconsistent with the extended conformation of the inhibitor on the enzyme. It suggests that modifications that will remove or distort important specific interactions with the enzyme, such as causing the loss of a hydrogen bond, are likely to result in a significant loss in binding energy and, hence, in the inhibitory activity. Such molecules can be rapidly excluded from the inhibitor design process with a model renin structure, allowing the chemists to focus on more productive modifications of the inhibitor structure.

1. General Considerations

A number of studies have been performed analyzing the range of interactions between an angiotensinogen substrate or related inhibitor peptide and the model renin active site. From these studies some of the details of the interacting groups have emerged, as well as knowledge of the relative contributions of the different residues in the inhibitors to the binding energy.

The interactions of the peptide analogs in Table 8 were examined in the Carlson renin model.[76-78] The structure-activity relationships of a number of renin inhibitors were analyzed by examination of the important intermolecular interactions determined by energy calculation. The peptides *8-2* to *8-5* (Table 8) were modeled in the active site in a conformation based on that of pepstatin in the rhizopuspepsin X-ray structure.[26] These complexes were minimized using CHARMM.[53] Molecular dynamics simulations were carried out on some of the complexes to study the average behavior of the inhibitors. The simulations were performed on the active-site region (all atoms within 10 Å of the inhibitor) with constraints on the rest of the enzyme. The structures obtained during the simulations were compared with the X-ray structure of peptide *8-1* in rhizopuspepsin.[32] The backbone conformation of the P_4-P_1' region was found to be similar in all the inhibitors. The hydrogen bonding interactions

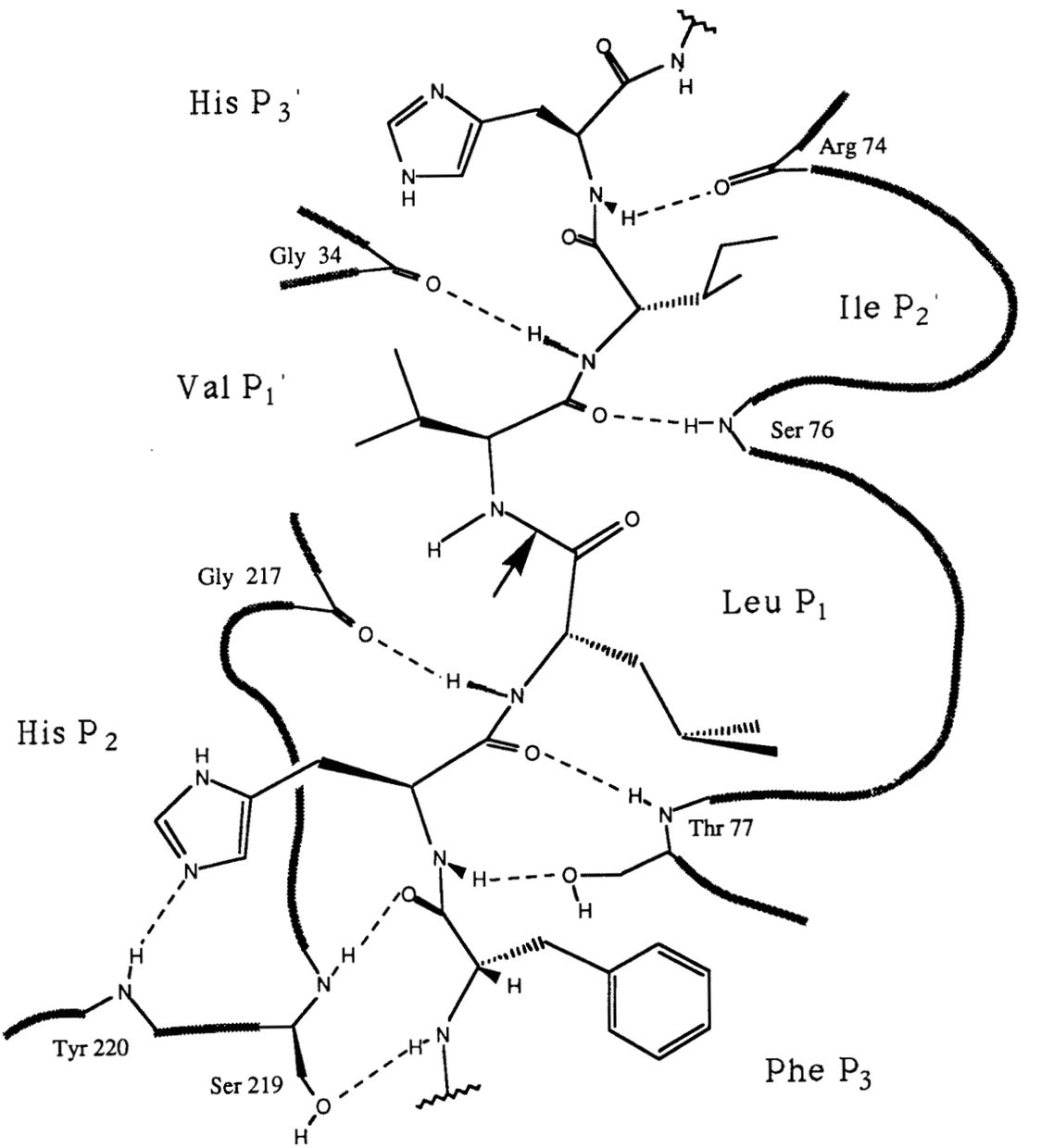

FIGURE 11. Schematic diagram of the renin substrate and the binding pocket residues on the human enzyme involved in hydrogen bonding between the main chain of the substrate and the enzyme. The scissile bond (arrow) is the amide bond cleaved in the hydrolysis. Many more hydrophobic interactions occur between the substrate and renin which are not shown in this figure.

between the inhibitor and the main chain of renin were also found to be similar to those in the crystal structure. The residues at P_5, P_3, and P_1 were found to bury at least half of their respective side chains in the corresponding pocket of renin. A comparison of the modeled inhibitors with a number of other renin inhibitors reported in the paper suggested the hydroxyethylene amide-bond replacement (Figure 5c) substituted for the transition state for amide-bond hydrolysis better than the reduced amide isostere (Figure 5d); peptide *8-7* was nearly 40 times more potent than the

TABLE 8
Renin Inhibitory Activities of C-Terminal Modified Inhibitors

		Renin inhibitory activity IC_{50} (n*M*)
1	D-His-Pro-Phe-His-Phe(CH_2NH)Phe-Val-Tyr	420
2	Ac-Ftr-Pro-Phe-His-Phe(CH_2NH)Phe-Val-Tyr-NH_2	3
3	Ac-Ftr-Pro-Phe-His-Phe(CH_2NH)Phe-NH_2	0.6
4	Ac-Ftr-Pro-Phe-His-Phe-Phe-Val-Ftr-NH_2	500
5	Ac-Ftr-Pro-Phe-His-Statine-Ile-NH_2	1.6
6	Ac-Ftr-Pro-Phe-His-Leu(CH_2NH)Val-NH_2	21
7	Ac-Ftr-Pro-Phe-His-Leu($CHOHCH_2$)Val-NH_2	0.6

Ac = acetyl.
Ftr = *N*-formyl-tryptophan.

reduced amide analog *8-6*. Cyclohexylmethyl and benzyl as side chains on the P_1 residue were found to provide more potent derivatives than either a leucine or phenylalanine side chain, due to a better fit in the hydrophobic P_1 pocket (see discussion of P_1 site below).

In a fundamental study,[35] a series of inhibitors was developed based upon the parent hexapeptide reduced amide inhibitor. Residues were removed systematically from both the N- and C-termini to try to establish which were essential for activity. A shorter inhibitor would simplify the structure and might overcome the obstacles of poor absorption, metabolic instability, and rapid biliary excretion of peptides. In anticipation of these studies, complexes of two hexapeptide reduced amide-bond inhibitors, *9-1* and *9-2* (Table 9), one with a His and the other with an Ala in the P_2 position, were minimized using VFFPRGs[61] in the original Abbott renin model. These minimized structures were used to rationalize the structure-activity relationships of a series of analogs of different lengths. The model studies showed that very specific hydrogen bonds were made between the main chain of residues P_3-P_1 and the enzyme (Figure 11). It was unlikely that these could be removed without significant loss of binding. This was exactly what was observed (Table 9). Removal of residues from the N-terminus of the hexapeptide led to completely inactive analogs in this series. The model structure showed, though, that few hydrogen bonds were made in the C-terminal portion of the inhibitor (Figure 11). Instead the major interactions were hydrophobic side chains P_1' and P_2' residing in hydrophobic subsites. P_3' seemed to have sev-

TABLE 9
Renin Inhibitory Activities of Reduced Amide-Bond Isosteres

		Renin inhibitory activity IC_{50} (n*M*)
1	Boc-Phe-His-Leu(CH_2NH)Val-Ile-His-OMe	300
2	Boc-Phe-Ala-Leu(CH_2NH)Val-Ile-His-OMe	980
3	Boc-His-Leu(CH_2NH)Val-Ile-His-OMe	>10,000
4	Boc-Leu(CH_2NH)Val-Ile-His-OMe	>10,000
5	Boc-Phe-His-Leu(CH_2NH)Val-Ile-OMe	2300
6	Boc-Phe-His-Leu(CH_2NH)Val-$NHCH_2Ph$	370
7	Boc-Phe-His-Cha(CH_2NH)Val-$NHCH_2Ph$	34
8	Boc-Phe-His-Cha(CH_2NH)Val-$NHCH_2CH(CH_3)C_2H_5$	7.8

Cha = cyclohexylalanine.

eral possible conformations, none of them particularly convincing. The structure-activity at the C-terminus fit the modeling very well. Residue P_3' was clearly dispensible (*9-1* vs. *9-5*), causing only an eightfold loss in activity. Furthermore, if the proper C-terminal hydrophobic group were used, (compare *9-6* and *9-7* to *9-5*), both P_3' and P_2' residues could be removed with no loss in activity relative to the parent compound.

The structure-activity relationship of a similar series of analogs, in this case based upon a statine transition-state analog (Table 10), was examined in the Carlson renin model.[79] Removing residues on the N-terminal side of the peptide caused a progressive loss of activity due to the loss of multiple hydrogen bonding and hydrophobic contacts between the inhibitor and the enzyme. The presence of a charged amino terminus in the shorter peptides, *10-7*, was detrimental due to the lack of countercharges nearby in the enzyme. There was also no space for solvation of the N-terminal amino group by water. Extension of the peptide in the N-terminal direction moved the positive charge further away from the active site (*10-5*, *10-6*) and led to improved activity.

A series of peptides, with the reduced amide-bond isostere at the cleavage site, was individually examined in the Carlson renin model (Table 11).[80] After energy refinement of each complex, a molecular dynamics simulation was carried out to observe the behavior of the inhibitor in the enzyme. The inhibitor was removed from the complex, and other likely conformations of the isolated peptide in the solution state were generated by a torsion-angle systematic-search procedure. These conformations were minimized using a solution-like environment (a dielectric of 80 and reduced hydrogen bonding force constants). The most probable conformation was found to be an extended peptide. The simulations of the inhibitor in the enzyme and in the solution-like environment were found to be consistent with the fluorescence energy transfer measurements of the end-to-end distance of the peptide in solution. The indole ring of the P_5 Trp and the phenyl ring of the P_3' Tyr were found to be approximately 16.5 Å apart. This suggested the peptides also existed, in solution, in an extended conformation. The simulations of the inhibitors in the model reflected a similar conformation to that in solution, with only the side-chain angles being altered significantly.

2. Scissile Bond Modifications

a. Comparison of Modifications

The Carlson model was used to attempt to

TABLE 10
Renin Inhibitory Activities of Statine Analogs

		Renin inhibitory activity IC_{50} (n*M*)
1	Pro-His-Pro-Phe-His-Phe-Phe-Val-Tyr-Lys	5200
2	Pro-His-Pro-Phe-Arg-Phe-Phe-Val-Tyr-Lys	200,000
3	Pro-His-Pro-Phe-His-Statine-Val-Tyr-Lys	10
4	Pro-Ftr-Pro-Phe-His-Statine-Ile-Ftr-NH_2	16
5	Pro-His-Pro-Phe-His-Statine-Ile-Phe-NH_2	3
6	Pro-Phe-His-Statine-Ile-Phe-NH_2	220
7	Phe-Statine-Ile-Phe-NH_2	>100,000
8	Pro-His-Pro-Phe-His-ACHPA-Ile-Phe-NH_2	30
9	Pro-His-Pro-Phe-Lys-ACHPA-Ile-Phe-NH_2	3900
10	Pro-His-Pro-Phe-His-AHPPA-Val-Tyr-Lys-NH_2	27

ACHPA — see Figure 14.
AHPPA — see Figure 14.
Ftr = *N*-formyl-tryptophan.

TABLE 11
Renin Inhibitory Potencies of Reduced Amide Isosteres

		Renin inhibitory activity IC_{50} (n*M*)
1	Ac-Ftr-Pro-Phe-His-Phe[CH_2NH]Phe-Val-Tyr-NH_2	3
2	Ac-DFtr-Pro-Phe-His-Phe[CH_2NH]Phe-Val-Tyr-NH_2	200
3	Ac-Trp-Pro-Phe-His-Phe[CH_2NH]Phe-Val-Tyr-NH_2	15
4	Ac-Pro-Phe-His-Phe[CH_2NH]Phe-Val-Tyr-NH_2	80
5	Ac-Ftr-Pro-Phe-His-Phe[CH_2NH]Phe-Val-NH_2	62

Ftr = *N*-formyl tryptophan.

correlate the energy of the enzyme-inhibitor complex with the renin inhibitory potency.[81] A peptide with the sequence of human angiotensinogen from residues His P_2 to His P_3' was constructed in the renin model and the energy of the complex partially minimized. The same procedure was followed with a series of inhibitors, varying only in the transition-state isostere used at the scissile bond of the substrate, including reduced amide, hydroxyethylene, and statine moieties (Table 12). The components of the interaction energy were examined by subtracting the individual energy components of the enzyme and of the inhibitor from the energy components of the enzyme-inhibitor complex.

$$\Delta E = E_{complex} - E_{enz} - E_{inh}$$

The authors concluded the alcohol transition-state isosteres bound efficiently due to a reduction in conformation strain relative to the natural substrate. Favorable electrostatic interactions between the alcohol moiety and the catalytic aspartic acids of the enzyme also played an important role. However, the exact energetics values were highly dependent on the precise structure of the complex. Similar efforts that were initiated using our own Abbott models to rationalize the structure-activity results of several series of compounds by an energetics analysis have never yet proven successful.

b. Dihydroxy Isosteres

A number of groups have developed dihydroxyethylene, or glycol, transition-state mimic analogs for renin based on early reports by Matsueda[82] and Hanson.[83] Some of these have been examined in renin models. The structures of several glycol inhibitors were minimized in the active site of the early Abbott renin model to investigate the effect and importance of the second hydroxyl group (Tables 13 and 14).[84] The renin inhibitory potency of the inhibitors increased by as much as 100-fold with the addition of a second hydroxyl group (*13-1* vs. *13-2*). The magnitude of the effect depended on the ster-

TABLE 12
Analogs Used in Energy Component Analysis

		Renin inhibitory activity IC_{50} (n*M*)
1	His-Pro-Phe-His-Leu-Val-Ile-His	300,000
2	His-Pro-Phe-His-Leu[CH_2NH]Val-Ile-His	200
3	His-Pro-Phe-His-Statine-Ile-His	20
4	His-Pro-Phe-His-Leu[$CHOHCH_2$]Val-Ile-His	3

TABLE 13
Comparison of Hydroxyethylene and Glycol Isosteres

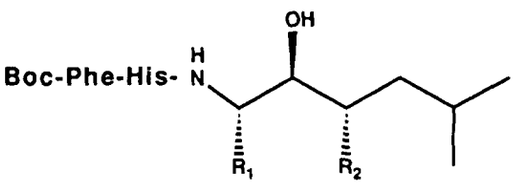

	R_1	R_2	Renin inhibitory activity IC_{50} (n*M*)
1	Isobutyl	H	1500
2	Isobutyl	OH	11
3	Cyclohexylmethyl	H	10
4	Cyclohexylmethyl	OH	1.5

eochemistry of the second hydroxyl group and on the alkyl group at the P_1 site. Molecular dynamics simulations of a number of inhibitors in the model were carried out to observe the behavior of the second hydroxyl group. The first hydroxyl remained between the two catalytic aspartic acids, while the second hydroxyl of the most active diasteromer *14-2* (R at C-3 and S at C-4) formed a hydrogen bond with Asp 215 in the active site (Figure 12a). When the alkyl group at P_1 was an isobutyl, the addition of the second hydroxyl with the S stereochemistry at C-3 gave a 100-fold increase in potency (*13-1* vs. *13-2*). However, when the alkyl group was a cyclohexylmethyl, only a factor of 7 increase in potency was seen (*13-3* vs. *13-4*). The conclusion was that when the alkyl group at the P_1 site of the inhibitor is isobutyl, the second hydroxyl can form the hydrogen bond with the aspartic acid side chain of the enzyme, thus restricting movement of the alkyl group in the P_1 site, allowing better dispersion interactions and better activity. When the alkyl group is a cyclohexylmethyl, the larger alkyl group more optimally fits the P_1 site, thus reducing the increase in potency upon addition of the second hydroxyl group. This was supported by the observation that the inhibitor with an isobutyl group was more mobile in the active site of renin during the molecular dynamics simulations than was the cyclohexylmethyl analog.

In a more recent study using the Abbott-new renin model, the glycol-based inhibitors were reexamined.[85] The structure-activity data showed the second hydroxyl was functioning as a hydrogen-bond acceptor. Modeling of these inhibitors

TABLE 14
Renin Inhibitory Activities of Glycol Diastereomers

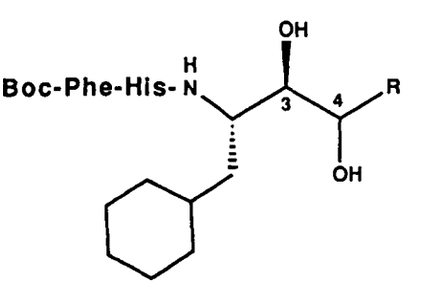

		Configuration at		Renin inhibitory activity IC_{50} (n*M*)
	R	3	4	
1	H	R	—	50
2	Isobutyl	R	S	1.5
3	Isobutyl	R	R	35
4	Isobutyl	S	S	70
5	Isobutyl	S	R	95

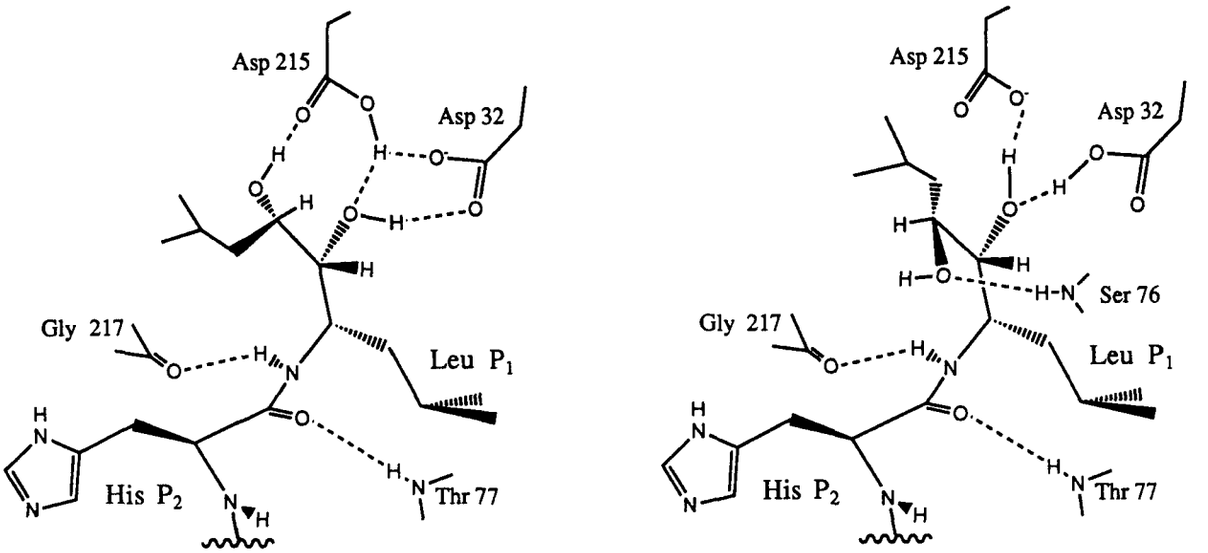

FIGURE 12. Two alternative conformations for the C-terminal glycol residue in renin inhibitors. (a) The hydroxyl mimicking the transition state is hydrogen bonded to the two catalytic aspartic acids. The second hydroxyl is bound to Asp 215.[84] (b) The first hydroxyl is in the same place as in (a), however, the second hydroxyl is now bound to the Ser 76 of the flap.[85,87]

in the Abbott-new renin model showed the second hydroxyl could accept a hydrogen bond from the amide hydrogen of Ser 76 (Figure 12b).

A series of inhibitors (Table 15) of very similar structure to those used above were designed to examine the effect of different alkyl groups at the P_1' position of the glycol inhibitors on renin inhibition.[83,86] Computer graphics showed alkyl substituents could fit into the P_1' subsite and activity should improve as the subsite became more occupied. Analogs with no alkyl group on the carbon bearing the second hydroxyl group had activity only in the micromolar range.[83] Addition of an alkyl side chain gave better renin inhibitors.[86] The best alkyl group in this series for the P_1' side-chain replacement was the isobutyl group (*15-5*), which would closely approximate the valine side chain at the P_1' position of human angiotensinogen. In other series, though, other alkyl groups give similar potency.[84]

The interactions of the second hydroxyl group were also examined.[87] Conformational analysis of an isolated acylated glycol residue showed a number of low-energy conformers that were characterized by an internal hydrogen bond between the (4S)-hydroxyl and the amide carbonyl of the P_2 residue. One of the low-energy conformations was used to build the structure of an inhibitor in the active site of the crystal structure of endoth-

TABLE 15
Activities of P_1' Alkyl Substituents

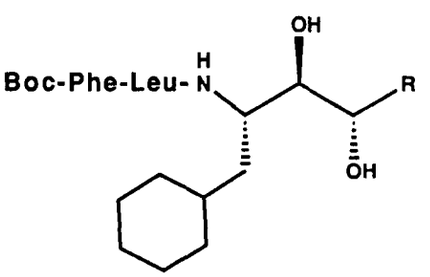

	R	Renin inhibitory activity IC_{50} (n*M*)
1	H	720
2	Methyl	190
3	Ethyl	210
4	Propyl	90
5	Isobutyl	60

iapepsin, which was used as a model of renin. The (3R)-hydroxyl was positioned between the two catalytic aspartic acids, and the cyclohexyl group was fitted into the P_1 pocket. This placed the second hydroxyl near the NH of Gly 76 of endothiapepsin (Figure 12b). The entire complex was then energy minimized. The authors concluded that the second hydroxyl of the glycol-based inhibitors mimics the P_1' carbonyl of angiotensinogen by accepting a hydrogen bond from the amide hydrogen of Ser 76 of the flap in renin (see Figure 11).

A different glycol dipeptide analog, shown in Table 16, was modeled in the Carlson renin model.[88] Examination of the structure of the inhibitor *16-1* in the model suggested the configuration of a hydroxyl introduced at C-3 in *16-2* should be R to allow this second hydroxyl group to interact with the Asp 215 side-chain carboxyl group at the catalytic site. The alkyl groups at the P_1 and P_1' sites were chosen to mimic the Leu-Val cleavage site of angiotensinogen. The resulting diol *16-3*, with R stereochemistry at C-3, was found to have activity comparable to the inhibitor without the second hydroxyl group, *16-2*. The other diastereomer was apparently not made. This result suggests the addition of the second hydroxyl group with the R configuration does not make additional binding interactions with renin. In the earlier study examining the stereochemistry of glycol inhibitors (Table 14), it was the S stereochemistry of the additional hydroxyl group that was found to have the best potency (*14-3*).

There are two differing hypotheses described for the likely conformation of the P_1' glycol res-

TABLE 16
Comparison of Transition-State Analogs

	Renin inhibitory activity IC_{50} (n*M*)
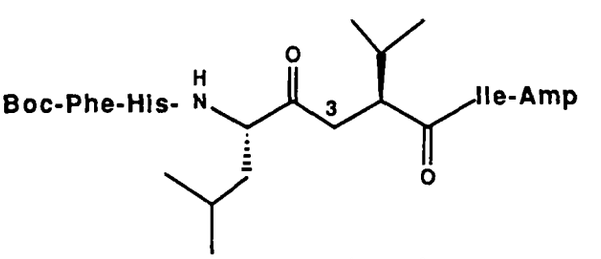	3.1
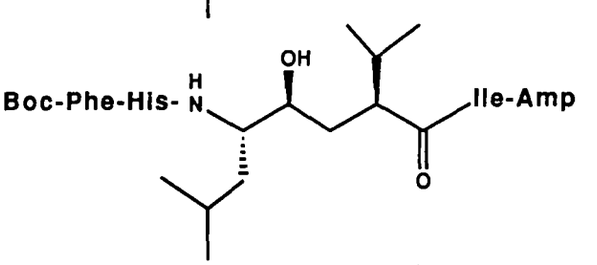	0.2
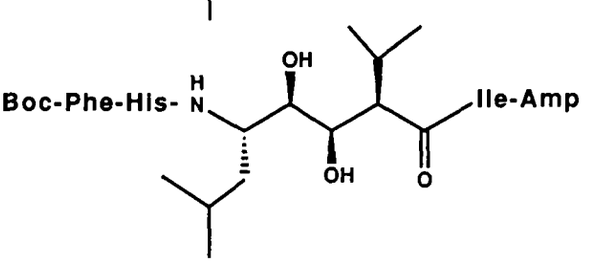	0.35

Amp = 3-aminomethylpyridine

idue. The first hydroxyl group is positioned between the catalytic aspartic acids. The second hydroxyl may interact either with Asp 215[84,88] or with Ser 76.[85,87] The question may be resolved with an X-ray structure of a glycol-based inhibitor in renin.

3. Modification at P_3

Using the glycol transition-state mimic, a large number of analogs were prepared with a number of different P_3 and P_4 residues to attempt to diminish the susceptibility of the Phe-His bond of the inhibitors to hydrolysis by chymotrypsin while maintaining renin inhibitory potency (Table 17).[89] A few of these compounds were modeled in the first Abbott renin model and in the chymotrypsin crystal structure. The modeling showed some analogs could fit reasonably well into the renin P_3 site, while not being able to fit well into the chymotrypsin active site. The phenylalanine at P_3 of the inhibitors was modified either by replacement of the nitrogen with other atoms or by modification of the side chain to prevent good binding of the side chain into the hydrophobic pocket of chymotrypsin. The half-lives for chymotrypsin hydrolysis of these inhibitors were extended while maintaining excellent renin inhibitory activity. The narrow chymotrypsin hydrophobic pocket could not tolerate the β,β-dimethyl-Phe (*17-4*) or the larger *O*-methyl-Tyr (*17-3*). Dehydro-Phe (*17-5*) also gave hydrolytically stable analogs, since the aryl ring would severely overlap with the residues of the chymotrypsin pocket. This modeling exercise showed how one could use structures of different enzymes to design compounds that would maintain important interactions with one enzyme but not interact well with another enzyme.

A series of compounds with longer *in vivo* half-lives were designed by making peptide backbone modifications.[90] It had been shown earlier[91] that *N*-methyl His at P_2 could give potent inhibitors, suggesting the NH is not involved in a critical hydrogen bond. Inspection of the inhibitor in the Carlson model showed the *N*-methyl N-C bond of a *N*-methyl His at P_2 and the α-carbon C-H bond of the residue at P_3 were nearly eclipsed (Figure 11) and could be replaced by a γ-lactam with minimal distortion of the backbone conformation. This modification could lead to potent inhibitors by giving conformational rigidity to the N-terminal portion of the inhibitor and could increase metabolic stability by making the inhibitors less susceptible to amide-bond hy-

TABLE 17
Comparison of Renin Inhibitory Activity and Chymotrypsin Hydrolysis Stability of P_3 Substitution

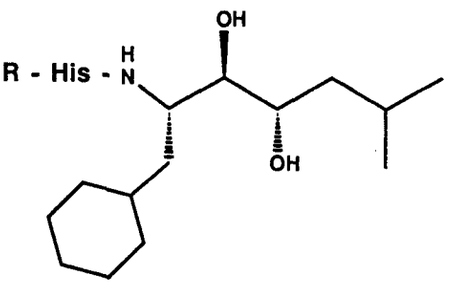

	R	Renin inhibitory activity IC_{50} (n*M*)	Chymotrypsin hydrolysis $t_{1/2}$ (min)
1	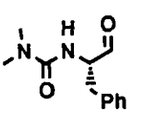	0.5	17.5
2	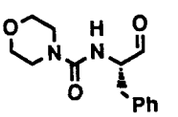	0.35	2.2
3	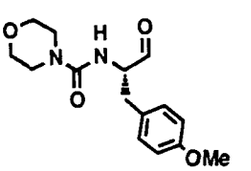	0.76	727
4	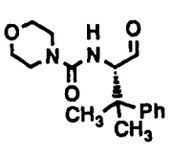	0.58	Stable
5	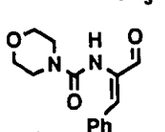	2.6	Stable
6	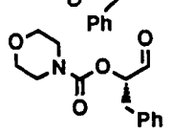	0.82	233

drolysis by chymotrypsin, for example. The modification was made in two series of transition-state mimic inhibitors (Table 18). In the statine series (*18-1, 18-2*), the renin inhibitory potency decreased by 100-fold upon incorporation of the lactam ring. Potency was also decreased for inhibitors upon *N*-methylation of the P_2 His residue.[91] In the hydroxyethylene series (*18-3* to *18-6*), the lactam analog either had the same or a modest (4x) increase in potency. These results suggest that peptides of the hydroxyethylene series may bind in a different manner than the statine analogs when the P_2 amide bond nitrogen is methylated or constrained in a lactam ring.

Two series of inhibitors with cyclic residues at P_3 were prepared based on a renin model developed at Merck that has not yet been published.[92] These peptides had a modified P_3-P_2

TABLE 18
Renin Inhibitory Activities of P_3 Lactam Analogs

X-Nle-Y-Ile-Amp

X	Y	Renin inhibitory activity IC_{50} (n*M*)
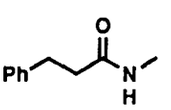	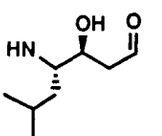	350
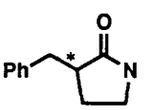	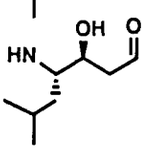	~10000[a] ~10000[a]
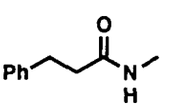	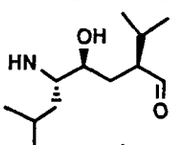	12
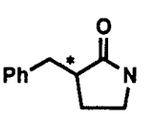	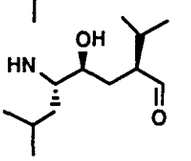	27[a] 14[a]
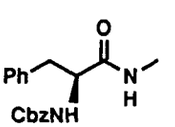	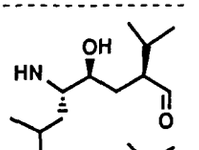	26
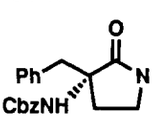	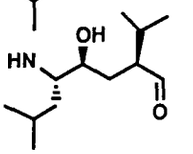	6.5

[a] Individual diastereomers.

Amp = 3-aminomethylpyridine.

amide bond and had the P_3 benzyl side chain bridged to the main chain (Table 19). The more conformationally rigid carbocyclic series (*19-1* to *19-3*) was weakly active. In the other series, one diastereomer, *19-6*, was relatively active. However, this was not the diastereomer that was predicted to be active based on the renin model. The renin model suggested the S stereochemistry at the carbon bearing the phenyl ring (3-position) would afford the best renin inhibitory potency. Therefore, their renin model is being adjusted to accommodate these results.

The P_3-P_2 amide bond has been replaced by a large number of isosteres (Table 20).[93,94] The activity of this series of inhibitors was examined using the Blundell renin model. One of the important interactions between renin and the inhibitors is the hydrogen bond from the amide hy-

TABLE 19
Renin Inhibitory Activities of P_3 Lactams

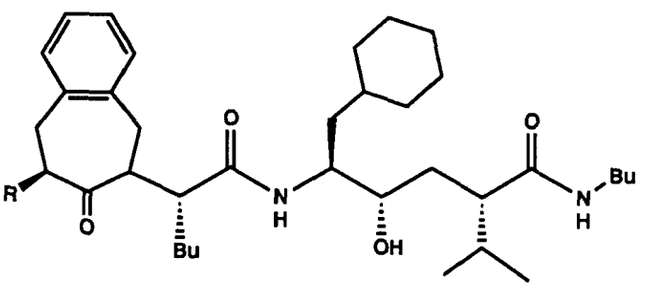

	R	Renin inhibitory activity IC_{50} (n*M*)
1	NH_2	2040
2	BocNH	1730
3	AcNH	210

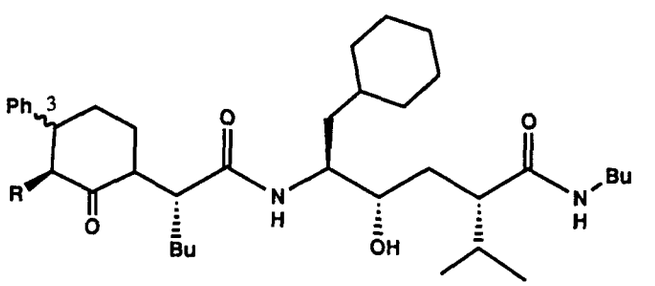

	R	Configuration at 3	Renin inhibitory activity IC_{50} (n*M*)
4	N_3	R	2300
5	BocNH	R	134
6	AcNH	R	21
7	N_3	S	1001
8	BocNH	S	5910

TABLE 20
Renin Inhibitory Activities of P_3-P_2 Amide Bond Modifications

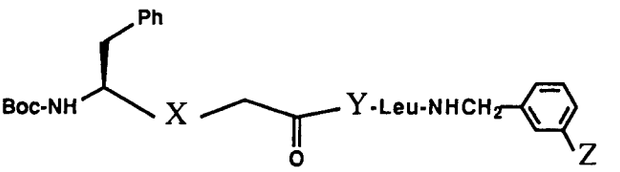

	X	Y	Z	Renin inhibitory activity IC_{50} (n*M*)
1		Sta	H	1100
2		Sta	H	>100,000
3	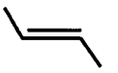	Sta	H	7000
4		Sta	H	21000
5		Sta	H	>100,000
6		ACHPA	H	530
7	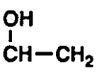	ACHPA	CH_2NH_2	20

Sta = Statine.
ACHPA — see Figure 14.

drogen of Ser 219 to the P_3 carbonyl of the inhibitor (Figure 11). The most potent inhibitors were those with a hydrogen-bond acceptor in an acceptable configuration. The hydroxyethylene analog *20-7* was found to be the most potent inhibitor, presumably because this hydrogen bond between the inhibitor and renin is best maintained.

4. Modification at P_2

Few results have been reported on modeling of inhibitors that vary at the P_2 residue. Inhibitors with a His residue at P_2 appear to have optimum potency and selectivity for human renin. The im-

provement in renin activity of a P_2 His residue over other residues at that position has been ascribed to two effects. It was found from molecular dynamics studies with the original Abbott model that the His side chain fills the P_2 volume better than a methyl group of an Ala analog.[95] The larger P_2 side chain reduced the mobility of the inhibitors in the active site, fostering better dispersion interactions and improving inhibitory activity (Table 9).

The His at P_2 of a ligand can also accept a hydrogen bond from the amide hydrogen of Tyr 220.[79] Inhibitors with basic residues, either a lysine or arginine, at P_2 were examined in the Carlson renin model (Table 21). Both had a dramatic loss of activity relative to their His analogs. The Carlson renin model showed there were no appropriate residues in the renin subsite that could neutralize the positive charge of these basic P_2 side chains. Because of the longer lengths of the Lys and Arg side chain, a hydrogen bond could not be formed between these residues and Tyr 220.

5. Modification at P_1

Using the rhizopuspepsin-pepstatin complex crystal structure[26] as a model for the renin interactions, Boger[96] suggested that in the statine-based inhibitors there is a large, unfilled hydrophobic area near the methyl groups of the statine side chain (Figure 13). It was felt that if this area could be filled, additional hydrophobic interactions would occur and the inhibitors would bind to renin more tightly. The Phe analog (AHPPA, Figure 14) could fill much of this volume, however, it appeared that the phenyl ring would not be recognized well by the leucine-specific recognition sites of renin. A cyclohexyl group, instead of the benzene ring, would keep the aliphatic nature of the side chain and add three hydrophobic methylene groups. Introduction of ACHPA (Figure 14) into the renin inhibitors gave an improvement of 60- to 70-fold in the renin inhibitory potency (Table 22). Ironically, the same substitution on the original model structure, rhizopuspepsin, gave relatively little improvement.[96] Using ACHPA as a core residue, other residues in the inhibitors have been varied, eventually developing inhibitors with subnanomolar potencies. However, inhibitors based on ACHPA are, in general, relatively insoluble. A number of attempts have been made to incorporate groups at either the N- or C-terminal residues to render the peptides more water soluble.[91,97] For the most part, these modifications have not led to significantly better renin inhibitory activity. Notwithstanding the solubility problems, ACHPA has become one of the standard residues to use as a transition-state analog.

A series of glycol analogs with different P_1 side chains were prepared in an effort to further optimize the side chains at the P_1 site.[95] In this series, the cyclohexylmethyl side chain continued to give the highest potency (Table 23). The benzyl and isobutyl analogs were weaker inhibitors, and other analogs, generally with larger side chains at P_1, were either very poor inhibitors or did not bind to renin at all. The inhibitors were modeled in the initial Abbott model, and the active-site region was minimized and subjected to

TABLE 21
P_2 Variation and Renin Inhibitory Potency

		Renin inhibitory activity IC_{50} (n*M*)
1	Pro-His-Pro-Phe-His-AHPPA-Ile-Phe-NH_2	30
2	Pro-His-Pro-Phe-Lys-AHPPA-Ile-Phe-NH_2	3900
3	Pro-His-Pro-Phe-His-Phe-Phe-Val-Tyr-Lys	5200
4	Pro-His-Pro-Phe-Arg-Phe-Phe-Val-Tyr-Lys	200,000

AHPPA — see Figure 14.

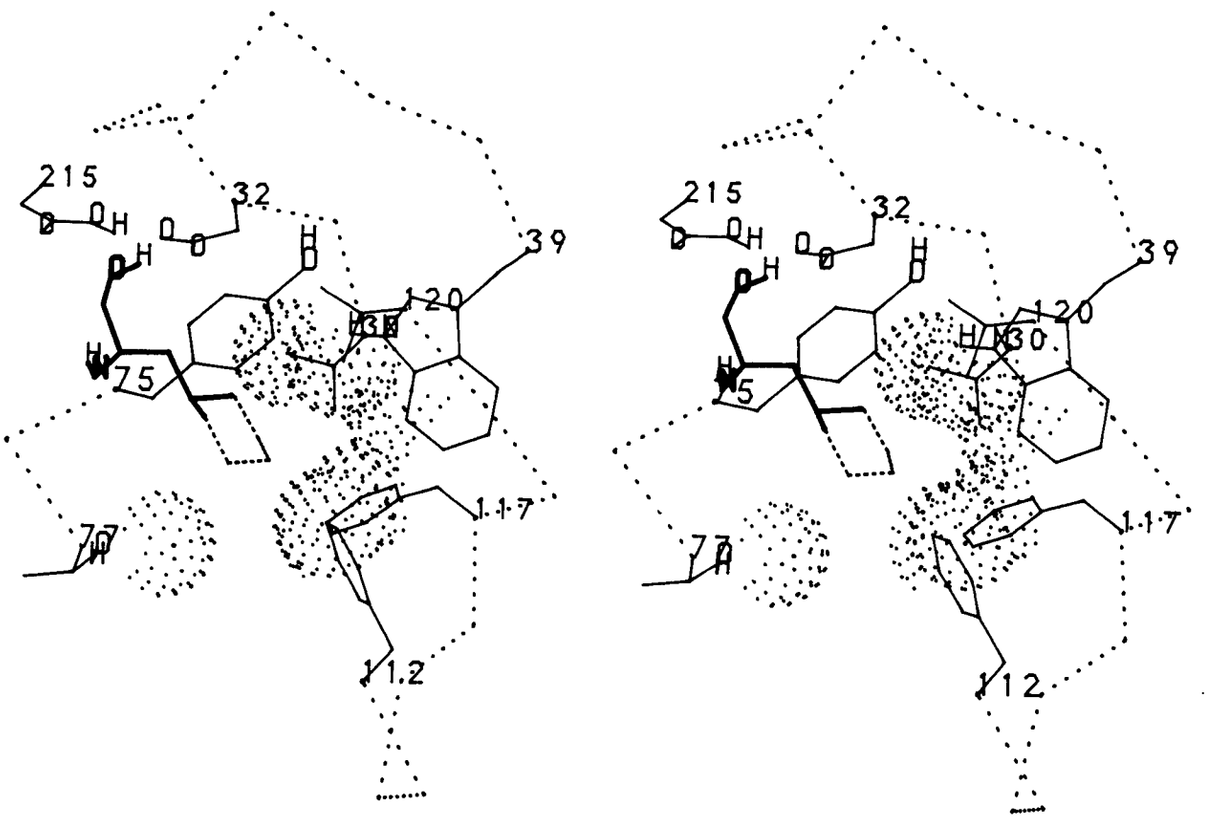

FIGURE 13. The P_1 Leu of human angiotensinogen leaves space between the Leu side chain and the residues lining the P_1 binding subsite. The three additional atoms of a cyclohexylalanine side chain (short dash) can fill the space more fully, resulting in an increase in van der Waals interactions.

molecular dynamics simulation to investigate the behavior of the respective side chains. The modeling results showed the cyclohexylmethyl optimally fitted the hydrophobic pocket of the P_1 area (Figure 13); the benzyl group fit slightly less well. The smaller isobutyl side chain did not fill the pocket, therefore, the dispersion energy was less and the inhibitor bound less well. The cyclohexyl, cyclohexylethyl, and other larger P_1 side chains caused large distortions in the enzyme structure and in the inhibitor, clearly showing why these are very poor inhibitors. Some of the largest side chains could not be modeled at all in the active site without severe steric overlaps.

The two methyl groups on the end of the side chain of the leucinol transition-state analog *24-1* were individually replaced by trifluoromethyl groups (Table 24).[98] The trifluoromethyl groups in these compounds would occupy different regions of the P_1 pocket (Figure 15) and interact with different residues lining the pocket. If the trifluoromethyl groups were able to stabilize a particular interaction, relative to the methyl group, the renin inhibitory activity should improve. The compounds were prepared and the potency of the 4S isomer (*24-2*) was four times the potency of the 4R analog (*24-3*). The structure of the inhibitor was modeled in the Akahane model of Iva-Val-Val-Sta-OEt/renin complex. The causes of the slight difference in activity between the diastereomers were difficult to determine. The authors concluded one possible explanation may be that the 4S methyl group is more buried in the renin model than is the other methyl group. The difference in solvation energies of a methyl group and a trifluoromethyl group would favor burying the trifluoromethyl group. However, the difference in solvation energy is relatively small.[99] The increase in potency of the 4S analog *24-2* may also be due to a weak hydrogen bond between the trifluoromethyl group and the side-chain amide of Gln 13. The isomer *24-3* would direct a methyl

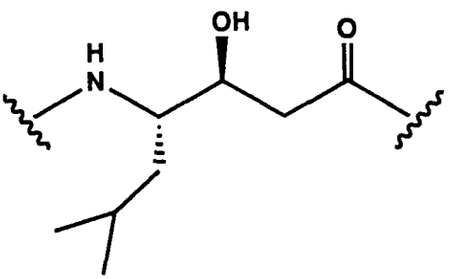

Statine

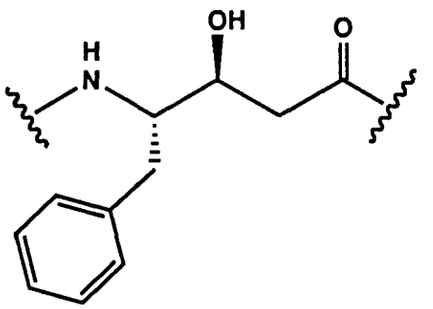

AHPPA
(4-Amino-3-hydroxy-5-phenyl
-pentanoic acid)

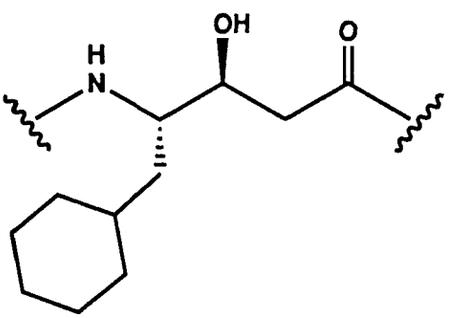

ACHPA
(4-Amino-5-cyclohexyl-3-
hydroxy-pentanoic acid)

FIGURE 14. Structures of residues used as P_1-P_1' transition state substitutes.

TABLE 22
Renin Inhibitory Activities of Inhibitors with Different P_1 Side Chains

Iva-His-Pro-Phe-His- X -Leu-Phe-NH_2

	X	Renin inhibitory activity IC_{50} (n*M*)	Rhizopuspepsin inhibitory activity IC_{50} (n*M*)
1	Sta	13	200
2	AHPPA	2.2	—
3	ACHPA	0.17	230

Sta = statine.
AHPPA — see Figure 14.
ACHPA — see Figure 14.

group toward the Gln 13 amide side chain. This could not form a hydrogen bond and would be less active. The reasons for the slight difference in renin activities are very subtle, and attempts to rationalize these small differences from model structures are fraught with difficulty.

6. Modification at P_1'

The statine-based inhibitors have been shown to generally have high renin inhibitory activity. Boger[96] and Powers[42] have suggested that statine acts as a dipeptide mimic, and this suggestion has been supported by structure-activity relation-

TABLE 23
Effect of P_1 Alkyl Substituents on Renin Inhibitory Activity

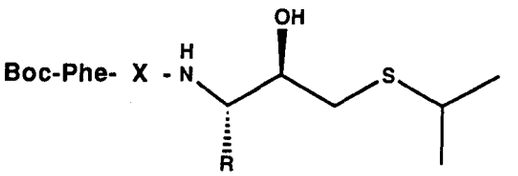

	X	R	Renin inhibitory activity IC_{50} (n*M*)
1	Ala	Isobutyl	700
2	His	Isobutyl	81
3	Ala	Cyclohexylmethyl	9
4	His	Cyclohexylmethyl	4
5	His	Cyclohexyl	150
6	His	Cyclohexylethyl	1500
7	His	Adamantylmethyl	2500
8	His	Benzyl	19
9	His	Benzhydryl	>10,000
10	His	Dicyclohexylmethyl	>10,000

ships. However, in the statine inhibitors there is no side chain corresponding to the P_1' Val side chain. Veber et al.[100] questioned whether potency could be further improved by addition of a 2-alkyl group on statine to occupy the P_1' pocket. Examination of a high-resolution X-ray structure of pepstatin in rhizopuspepsin[26] as a model for the interactions in renin showed the R configuration for an alkyl group at C-2 of the statine was required (Figure 16a). Synthesis of the (R)-2-isobutyl analog of statine (*25-4*) (Table 25) gave inhibitors with renin inhibitory potencies comparable to the unsubstituted congeners. Compound *25-5*, with the 2S configuration, had significantly lower activity. However, although the modeling, which was done using rhizopuspepsin, indicated alkyl substituents at C-2 of statine should improve activity, the rhizopuspepsin inhibitory activity of *25-4* and *25-5* was worse than any of the unsubstituted reference inhibitors. Molecular modeling[2] showed that for larger peptides with a Phe at position P_3', the phenyl ring may occupy a portion of the P_1' site and may partially com-

TABLE 24
Activities of P_1' Trifluoromethyl-Substituted Leucinal Diastereomers

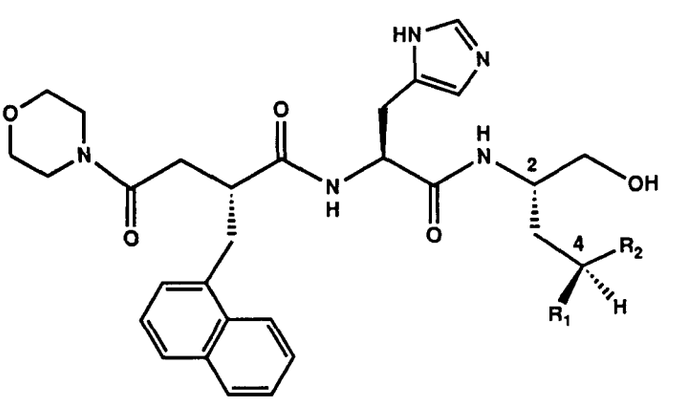

	R_1	R_2	Configuration at 2	Configuration at 4	Renin inhibitory activity IC_{50} (n*M*)
1	CH_3	CH_3	S		1300
2	CH_3	CF_3	S	S	570
3	CF_3	CH_3	S	R	2600
4	CH_3	CF_3	R	S	>10,000
5	CF_3	CH_3	R	R	>10,000

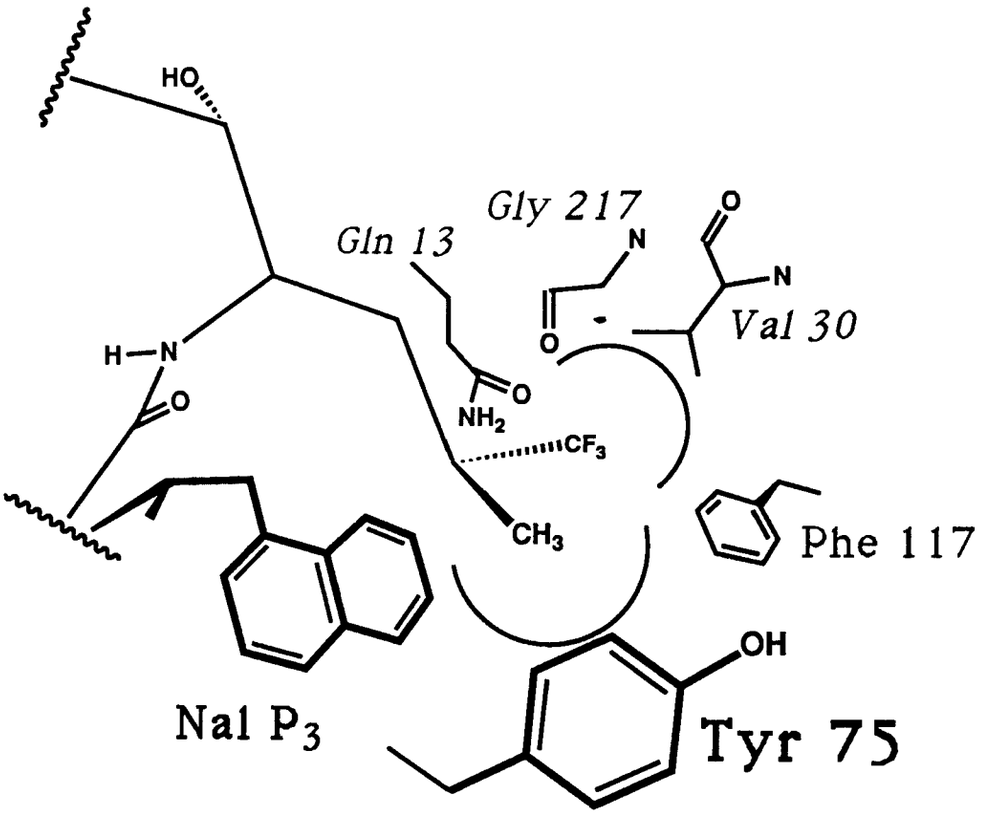

FIGURE 15. Schematic diagram showing the different environments created by the residues neighboring the 4S-trifluoro analog of the Leu P_1 residue in the Akahane model. The different environments could affect the potency of the different trifluoromethyl analogs (Table 24).

pensate for the missing P_1' side chain in the unsubstituted analog. This would explain why the addition of the alkyl group in this series did not provide a dramatic increase in potency. In a shorter series of peptides, Boc-Phe-ACHPA-sec-pentylamide, the 2-position of ACHPA was substituted by an allyl group.[101] The 2-allyl substitution generally increased the potency of the inhibitors.

Norstatine has been used as a statine replacement (Figure 5b).[102] Norstatine inhibitors (Table 26) were found to fit well in the Akahane model. The hydrogen-bonding network between the enzyme and the main chain of the inhibitor was maintained, the hydrophobic P_1 and P_3 side chains fit into the hydrophobic areas of the enzyme, and the alkyl ester group of the norstatine could mimic the Val P_1' side chain of angiotensinogen (Figure 16b). The norstatine inhibitor *26-1* was found to be seven times more potent than the statine analog *26-4*, presumably due to a better fit of the isopropyl ester into the P_1' site of the enzyme. This series of compounds may be considered as either a dipeptide analog that is two atoms shorter than a natural dipeptide or, perhaps more accurately, as an amino acid with one extra atom. With the hydroxyl group acting as a transition-state mimic and situated between the catalytic aspartic acid side chains, the carbonyl group would be moved closer to the P_1' site. The ester group would then be in a position to interact more favorably with the P_1' pocket.

7. C-Terminal Modifications

A number of tripeptide analogs have been prepared by replacing the C-terminal amide bond of the hydroxyethylene dipeptide mimic with an amide-bond replacement (Table 27).[103] Exami-

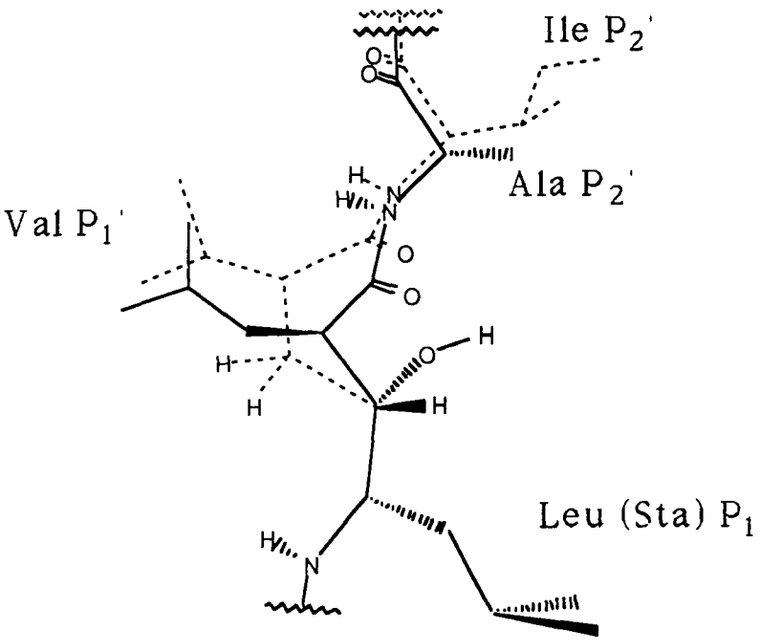

A

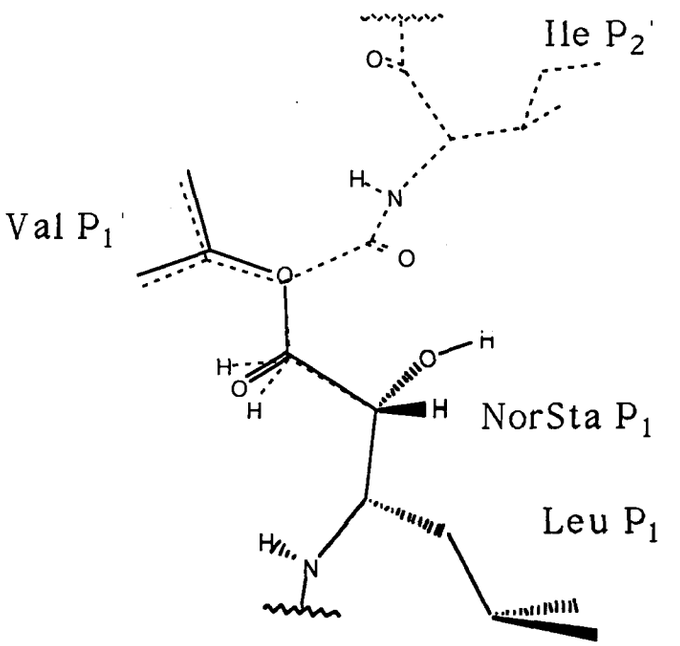

B

FIGURE 16. Schematic figures showing inhibitor modifications designed to interact with the P_1' binding site. (a) Overlap of (R)-2-isobutylstatine (solid) with a hydroxyethylene isostere (dotted) showing how the P_1' site could be filled by the alkyl group on statine. (b) Overlap of a norstatine ester analog (solid) with the hydroxyethylene transition state analog (dotted). The alkyl group of the ester occupies the P_1' site.

TABLE 25
Renin Inhibitory Activity of 2-Alkyl Statine Analogs

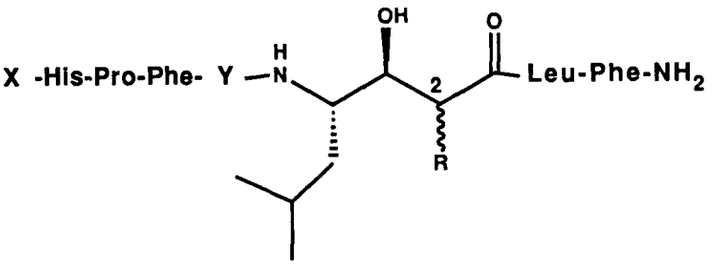

	X	Y	R	Renin inhibitory activity K_i (n*M*)	Rhizopuspepsin activity K_i (n*M*)
1	Isobutyl	His	H	7.7	230
2	Boc	His	H	2.3	110
3	Boc	Phe	H	0.8	220
4	Isobutyl	Phe	(R)-isobutyl	1.7	1900
5	Isobutyl	Phe	(S)-isobutyl	120	1900

nation of the conformation of a long peptide inhibitor in the first Abbott renin model showed a hydrogen bond existed between the carbonyl of the P_1'-P_2' amide bond and the NH of Ser 76 on the flap of renin (Figure 11). The amide-bond replacements were chosen so this hydrogen bond would be conserved in the new inhibitors. A variety of alkyl groups interacting at the P_2' site of renin were examined in the renin model (Table 27). The conformation of the inhibitors was based on a model of a hexapeptide inhibitor in the enzyme. The positions of the alkyl groups were examined by energy minimization and molecular dynamics. Although the differences in activity are small when the P_1 side chain is isobutyl, the ketone and sulfone replacements gave better inhibitors. Presumably they were able to maintain the hydrogen-bonding interaction to the flap residue. Variation of the alkyl group on the sulfur (*27-5* to *27-7*) did not affect the activity dramatically. The isopropylsulfonyl group was found to mimic best the Ile P_2' side chain of angiotensinogen. As had been seen before,[96] substitution of the isobutyl side chain by a cyclohexylmethyl side chain at P_1, *27-8*, led to a 20-fold increase in inhibitory potency. A further increase in activity was seen when the alanine at P_2 was replaced with a histidine, *27-9*.

8. Cyclic Inhibitors

A number of attempts have been made to use molecular modeling methods and the renin model structures to develop cyclic renin inhibitors. These might have greater potency because of greater conformational rigidity and the potential of increased metabolic stability. In addition, changes in the shape of the inhibitor molecule might have an effect on bioavailability.

a. N-Terminal Cyclics

An early report by Paiva[104] indicated that renin inhibitors could be made by replacing the Ile at position P_6 and the Leu at P_1 (Figure 17a) with cysteines and forming the disulfide bond to create cyclic compounds. These compounds were found to be weak inhibitors of porcine renin (Table 28). Other similar cyclic compounds, incorporating a Pro-Phe β-turn, were also weak renin inhibitors.[105,106] These results were taken as support for the hypothesis that the P_5-P_2 region of angiotensinogen may have a β-turn-like conformation (Figure 17a).[105,106]

Molecular modeling indicated that a cyclic system, similar to Paiva's, could be made be-

TABLE 26
Norstatine Inhibitors

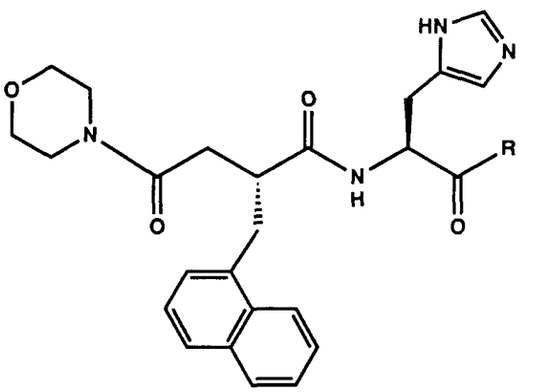

	R	Renin inhibitory activity IC_{50} (n*M*)
1	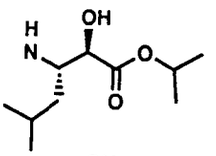	25
2	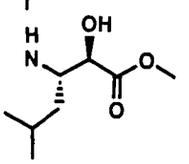	52
3	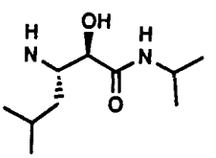	130
4	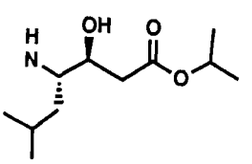	180

tween the side chains of the P_5 and P_2 residues (Figure 17b) and showed a 16-membered ring would be optimal (Table 29).[40,41] The 16-membered ring compound, *29-3*, was of comparable potency to the linear reference inhibitors, *29-1* and *29-2*, against porcine renin. Other ring sizes were at least six times less potent than the 16-membered ring compound. Energy calculations suggested a type I or type III β-turn would form at the Pro-Phe residues.

Analysis of these cyclic analogs on the renin model structures leads to the important conclusion that formation of a cyclic system by joining the side chains of the P_6 and P_1 or the P_5 and P_2 residues will cause the P_3 phenylalanine to move out of the binding subsite where it is usually placed. In the usual binding mode, the Phe P_3 side chain is placed in the corresponding subsite in the renin model where the side chain of the first Val side chain binds in the pepstatin-rhizopuspepsin structure (Figure 7).[26] However, in order to form the P_6-P_1 cycle, the Phe P_3 side chain would have to follow the Iva instead (Figure 17a). The two alternative structures result in a very different placement and orientation of all the residues N-terminal to P_3 (Figure 17a). Close examination of the β-turn P_6-P_1 cyclic structure on the renin model suggests that such a structure cannot fit into the active site. It requires that the β-strand, including Pro P_4, His P_5, and Ile P_6, pass through the active site between the flap and the Pro-Pro-Pro loop of residues 290 through 300 on renin adjacent to the strand containing P_3, P_2, and P_1 (see Figure 17a). The model renin structures do not provide sufficient room to fit this additional β-strand in the active site in a position where it could form a bridge from P_6 to P_1. This is especially true since the P_1 side chain is buried deep in the active site. These modeling considerations would explain why the P_6-P_1 cyclics are so very weak (Table 28). The P_5-P_2 cyclics, though, are much more potent (Table 29); the activity of the cyclic compound *29-3* of Table 27 is of the same order of magnitude as a linear analog. This result may be explained by a rather different structure for the cycle, shown schematically in Figure 17b, which does not assume the β-turn at the Phe-Pro and accommodates Phe P_3 in its usual subsite.

A number of cyclic inhibitors were prepared with the Phe-Phe cleavage site included in the ring (Table 30).[78] Only the 20-membered ring analog, *30-3*, containing a P_4 Cys and a P_2' Cys, was significantly active. Molecular modeling of the cyclic inhibitor in the Carlson model indicated a reverse-turn existed between the P_3 and P_1' residues. Replacement of the Phe-Phe by statine or the reduced amide-bond isostere did not give analogs with increased activity.

Inspection of the renin inhibitors in the early

TABLE 27
Renin Inhibitory Activities of C-Terminal Tripeptide Analogs

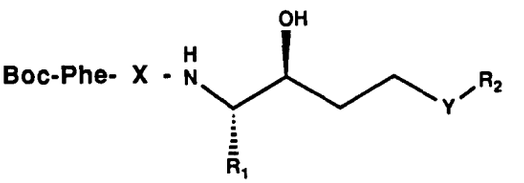

	X	R_1	Y	R_2	Renin inhibitory activity IC_{50} (n*M*)
1	Ala	Isobutyl	CO	Isopentyl	2400
2	Ala	Isobutyl	CHOH	Isopentyl	3800
3	Ala	Isobutyl	S	Isopentyl	5500
4	Ala	Isobutyl	SO	Isopentyl	5200
5	Ala	Isobutyl	SO_2	Isopentyl	2400
6	Ala	Isobutyl	SO_2	Isobutyl	3200
7	Ala	Isobutyl	SO_2	Isopropyl	1600
8	Ala	c-HexCH_2	SO_2	Isopropyl	76
9	His	c-HexCH_2	SO_2	Isopropyl	7.6

c-HexCH_2 = cyclohexylmethyl.

Abbott renin model showed that the side chain of the P_1 residue is close to the amide bond nitrogen of the P_2 residue and could be bridged to form cyclic inhibitors (Figure 18).[107] A number of potential cyclic inhibitors were modeled in the active site based on the conformation of pepstatin in the rhizopus enzyme and were minimized using VFFPRG[61] (Table 31). Significant changes occurred in the conformation of the flap of the renin model to accommodate the added bridging methylene groups. The 10-, 12-, and 14-membered ring compounds were prepared and the best inhibitor, the 14-membered compound *31-6*, was half as potent as the linear reference inhibitor *31-2* (Figure 18). From the perspective of the modeling, it was surprising that the 10-membered ring compound *31-4* was inactive. Therefore, the conformations of the isolated cyclic compounds were examined by NMR spectroscopy. These studies indicated that the 10-membered ring had a *cis* amide bond between the P_3 and P_2 residues. Molecular modeling of the 10-membered ring shows the *cis* amide bond inhibitor structure cannot fit in the renin model without major steric overlaps with the enzyme.[108] Only the *trans* isomer can bind to the active site. NMR spectroscopy showed the 12- and 14-membered ring analogs had two sets of signals, corresponding to two conformational states, the interconverting *cis* and *trans* amide bond isomers. The modeling shows the activity of these cyclic inhibitors is dependent on the amount of *trans* amide bond isomer present, the 14-membered ring has the highest percentage of *trans* isomer and has the best potency; the 12-membered ring, *31-5*, is intermediate between the 10- and 14-membered analogs in both percent *trans* isomer and renin inhibitory potency.

b. C-Terminal Cyclics

Modeling based on the rhizopuspepsin-pepstatin X-ray structure[26] showed a ring could be constructed from the P_2 residue side chain to the P_3' carboxy terminal residue, thus restricting the conformation of the intervening residues (Table 32).[40,41] Inhibitors with a cysteine or homocysteine substituted for the His at P_2 and disulfide

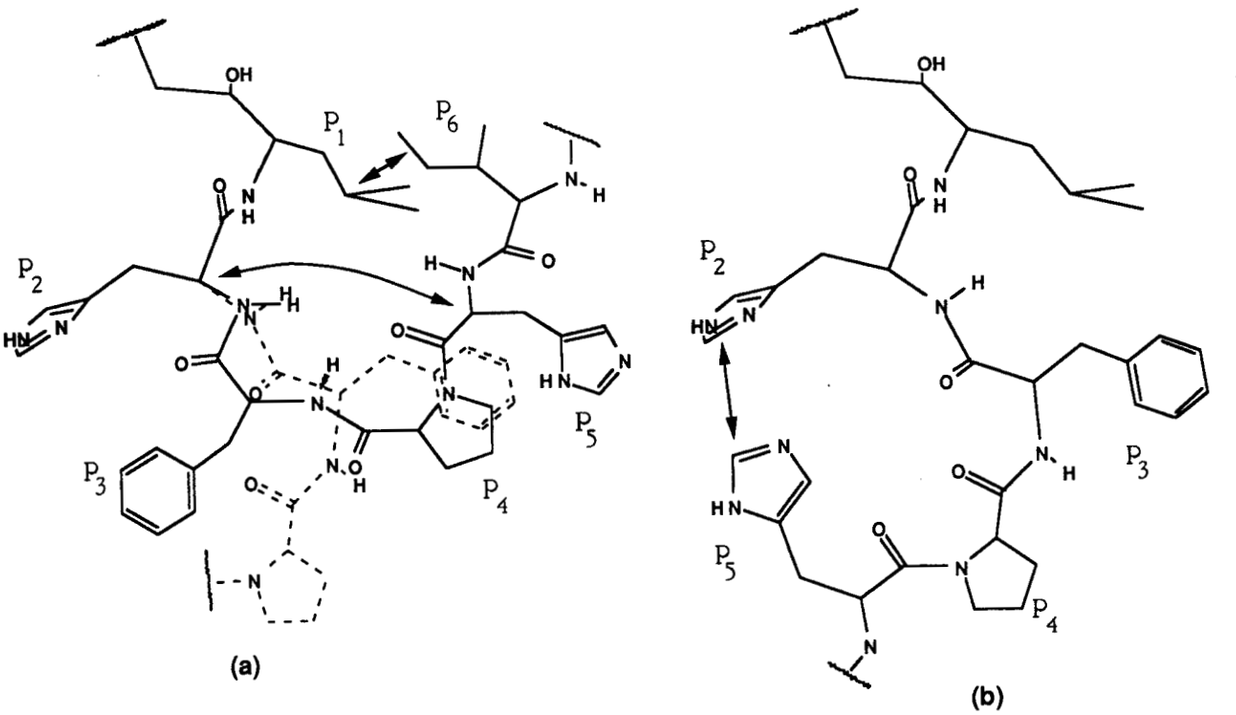

FIGURE 17. Alternate conformations for the P_6 to P_1 region of the substrate in the renin binding pocket. (a) Conformation required to form the P_6 to P_1 bridged analogs (solid)[104-106] containing a β-turn at P_3 and P_4. The arrows mark the P_6-P_1 bridge,[104-106] as well as a P_5-P_2 bridge.[40,41] This structure is compared to the usual conformation for the substrate (dashed). Note that the Phe P_3 side chain lies in very different positions in the two conformations. (b) An alternative conformation that could accommodate a P_5-P_2 bridge without having to move the Phe P_3 main chain or side chain from its usual binding site or invoke a β-turn at P_3-P_4.

TABLE 28
Renin Inhibitory Activities of P_6-P_1 Cyclic Inhibitors

		Porcine renin inhibitory activity (K_i (n*M*)
1	Cys-His-Pro-Phe-His-Cys-Leu-Val-Tyr Ser	17100
2	Cys-His-Pro-Phe-His-Cys-Leu-Val-Tyr-Lys	6900

cyclization with a thiol at the C-terminus were prepared. These were of comparable potency (2 to 3 times less active) to the linear analog *32-2*, with His replaced by Ala, which itself led to a substantial decrease in renin inhibitory potency (11-fold).

IV. CONCLUSIONS

While molecular modeling by homology has been in use now for close to 20 years, application of the methodology in a systematic way to study the functional properties of enzymes is relatively

TABLE 29
Renin Inhibitory Activities of P_5-P_2 Cyclic Inhibitors

		Porcine renin inhibitory activity K_i (n*M*)
1	His-Pro-Phe-His-Sta-Leu-Leu-Phe-NH_2	20
2	Abu-Pro-Phe-Abu-Sta-Leu-Phe-OCH_3	24
3	Hcy-Pro-Phe-Hcy-Sta-Leu-Phe-OCH_3	49
4	Hcy-Pro-Phe-Cys-Sta-Leu-Phe-OCH_3	280
5	Cys-Pro-Phe-Cys-Sta-Leu-Phe-OCH_3	2200

Hcy = homocysteine.
Abu = aminoisobutyryl.

TABLE 30
Renin Inhibitory Activities of Inhibitors Incorporating the Scissile Bond and its Replacements

		Renin inhibitory activity IC_{50} (n*M*)
1	Pro-His-Pro-Phe-His-Phe-Phe-Val-Tyr-Lys	8000
2	Ac-His-Pro-Phe-Cys-Phe-Phe-Cys-Ftr-NH_2	2900
3	Ac-Ftr-Cys-Phe-His-Phe-Phe-Cys-Ftr-NH_2	190
4	Ac-Ftr-Pro-Phe-Cys-Statine-Cys-Ftr-NH_2	1500
5	Ac-Ftr-Cys-Phe-His-Statine-Cys-Ftr-NH_2	4300
6	Ac-Ftr-Cys-Phe-His-Phe(CH_2NH)Phe-Cys-Ftr-NH_2	760

Ac = acetyl.
Ftr = *N*-formyl-tryptophan.

new. The use of such model structures in drug design is unfortunately still in its infancy. The major problem that is faced in the use of model structures is that most of the properties of interest in modeling are energy-determined or -controlled processes. For example, the potency of a renin inhibitor is clearly related to how well it binds to the renin active site, i.e., its free energy of binding ($\Delta G_{binding}$). The most serious limitation today is the inability to determine the energetics of protein structures or protein/ligand complexes with sufficient accuracy to calculate these properties. This limitation prevents us from properly refining our model structures to sufficient accuracy for evaluation of functional properties or inhibitor binding. It prevents us from calculating ligand binding and inhibitory constants that would allow us to correctly predict the inhibitory potency of novel compounds. Until such time as these energy calculations can be performed prop-

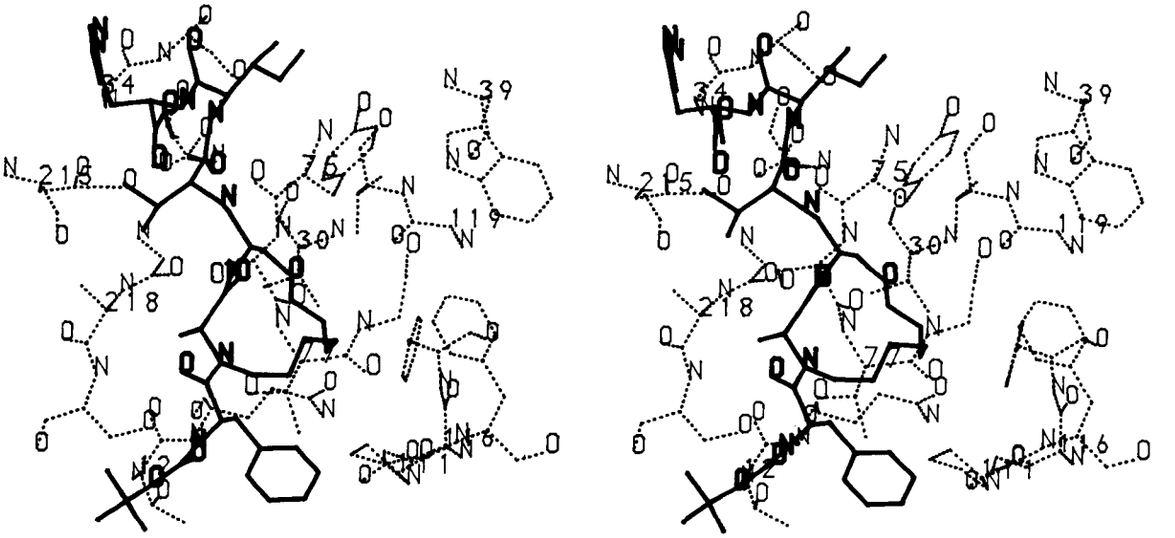

FIGURE 18. Conformation of the 14-membered cyclic inhibitor *31-6* (solid) in the original Abbott renin model (dotted).

TABLE 31
Renin Inhibitory Activities of P_2-P_1 Cyclic Inhibitors

		Renin inhibitory activity IC_{50} (n*M*)	% *trans*
1	Boc-Phe-His-Leu(CH_2NH)Val-Ile-His-OMe	280	100
2	Boc-Phe-Ala-Leu(CH_2NH)Val-Ile-His-OMe	1400	100
3	Boc-Phe-Ala-Leu(CH_2NH)Val-Ile-His-OMe CH_3	1200	100
4	Boc-Phe-Ala-Ser(CH_2NH)Val-Ile-His-OMe $L(CH_2)_3$	>100,000	0
5	Boc-Phe-Ala-Ser(CH_2NH)Val-Ile-His-OMe $L(CH_2)_5$	69,000	20
6	Boc-Phe-Ala-Ser(CH_2NH)Val-Ile-His-OMe $L(CH_2)_7$	2700	50

erly, the field of modeling will be largely reduced to qualitative, descriptive, even vague statements trying to rationalize the structure-activity *ex post facto*. This latter situation all too accurately describes much of the modeling literature on the renin structure.

Despite the serious limitations discussed above, modeling has had a significant impact on the design of novel renin inhibitors. It has provided the many chemists working in this area with a three-dimensional view of the active site and the conformation of the inhibitor when bound to the enzyme. It has produced a picture of the respective binding pockets for the side chains of the inhibitor and their relative spatial relationships. It has elucidated the specific interactions made by the inhibitor with the enzyme so that the chemist can preserve them while trying to add additional interactions or modifications that will increase such inhibitor properties as potency, metabolic stability, or oral bioavailability. It is most valuable in producing a three-dimensional structural environment in which the chemist can design novel structures tailored to fit the active

TABLE 32
Renin Inhibitory Activities of P_2-C-Terminal Cyclic Inhibitors

		Renin inhibitory activity K_i (n*M*)
1	Ibu-His-Pro-Phe-His-Sta-Leu-Phe-NH_2	7.7
2	Ibu-His-Pro-Phe-Ala-Sta-Leu-Phe-NH_2	99
3	Ibu-His-Pro-Phe-Cys-Sta-Leu-Phe-$NHCH_2CH_2S$	380
4	Ibu-His-Pro-Phe-Hcy-Sta-Leu-Phe-$NHCH_2CH_2S$	200

Ibu = isobutyryl.
Hcy = L-Homocysteine.

site, avoid modifications that do not fit, and attempt to prepare structures that would not be conceived without the structural framework.

The above comments indicate important areas for the future evolution of this field of molecular modeling and drug design. Methods need to be developed to improve our ability to refine the approximate model structures produced by comparative modeling. In the absence of adequate energetics methods, very careful attention and detailed inspection of the model structures by the molecular modeling experts are essential to avoid the many false local minima and serious errors in the structure. The determination of the crystal or NMR experimental structures of the protein and protein-ligand complex would partially solve this problem. Improvements in the treatment of protein energetics and solvent are also needed to permit sufficiently accurate calculations of the free energy of binding of ligands. Much effort is being expended in the field of protein energetics to try to solve these problems. Finally, a variety of methods[109-111] are being developed to allow us to use these structures and energetics to help arrive at novel, potent inhibitors. As these methods improve, the contribution of renin modeling to the design of new inhibitors and to our understanding of renin functional properties is likely to increase and become ever more important.

REFERENCES

1. **Wyvratt, M. J. and Patchett, A. A.,** Recent developments in the design of angiotensinogen-converting enzyme inhibitors, *Med. Res. Rev.*, 5, 483, 1985.
2. **Greenlee, W. J.,** Renin inhibitors, *Med. Res. Rev.*, 10, 173, 1990.
3. **Browne, W. J., North, A. C. T., Phillips, D. C., Brew, K., Vanaman, T. C., and Hill, R. L.,** A possible three-dimensional structure of bovine α-lactalbumen based on that of hen's egg-white lysozyme, *J. Mol. Biol.*, 42, 65, 1969.
4. **McLachlan, A. D. and Shotton, D. M.,** Structural similarities between α-lytic protease of Myxobacter 495 and elastase, *Nature New Biol. (London)*, 229, 202, 1971.
5. **Greer, J.,** Model for haptoglobin heavy chain based upon structural homology, *Proc. Natl. Acad. Sci. U.S.A.*, 77, 3393, 1980.
6. **Greer, J.,** Comparative model-building of the mammalian serine proteases, *J. Mol. Biol.*, 153, 1027, 1981.
7. **Greer, J.,** Protein structure and function by comparative model building, *Ann. N.Y. Acad. Sci.*, 439, 44, 1985.
8. **Feldmann, R. J., Bing, D. H., Potter, M., Mainhart, C., Furie, B., Furie, B. C., and Caporale, L. H.,** On the construction of computer models of proteins by the extension of crystallographic structures, *Ann. N.Y. Acad. Sci.*, 439, 12, 1985.
9. **Greer, J.,** Comparative modeling methods: appli-

cation to the family of the mammalian serine proteases, *Proteins*, 7, 1990, in press.

10. **Navia, M. A., Springer, J. P., Poe, M., Boger, J., and Hoogsteen, K.,** Preliminary X-ray crystallographic data on mouse submaxillary gland renin and renin-inhibitor complexes, *J. Biol. Chem.*, 259, 12714, 1984.
11. **Morris, B. J., Catanzaro, D. F., Hardman, J., Mesterovic, N., Tellam, J., Hort, Y., Bennetts, B. H., and Shine, J.,** Structure of human renin and expression of the renin gene, *Clin. Exp. Pharmacol. Physiol.*, 11, 369, 1984.
12. **Sielecki, A. R., Hayakawa, K., Fujinaga, M., Murphy, M. E., Fraser, M., Muir, A. K., Carilli, C. T., Lewicki, J. A., Baxter, J. D., and James, M. N.,** Structure of recombinant human renin, a target for cardiovascular-active drugs, at 2.5 Å resolution, *Science*, 243, 1346, 1989.
13. **Umezawa, H., Aoyagi, T., Morishima, H., Matsuzaki, M., Hamada, M., and Takeuchi, T.,** Pepstatin, a new pepsin inhibitor produced by actinomycetes, *J. Antibiot.*, 23, 259, 1970.
14. **Gross, F., Lazar, J., and Orth, H.,** Inhibition of the renin-angiotensinogen reaction by pepstatin, *Science*, 175, 656, 1972.
15. **Miller, R. P., Poper, C. J., Wilson, C. W., and DeVito, E.,** Renin inhibition by pepstatin, *Biochem. Pharmacol.*, 21, 2941, 1972.
16. **Corvol, P., Panthier, J. J., Soubrier, F., Menard, J., and Rougeon, F.,** Mouse submaxillary renin: a useful model for the study of renal renin, *J. Hypertens. Suppl.*, 1, 3, 1983.
17. **Misono, K. S., Chang, J. J., and Inagami, T.,** Structure of mouse submaxillary gland renin, *Clin. Exp. Hypertens. [A]*, 5, 941, 1983.
18. **Imai, T., Miyazaki, H., Hirose, S., Hori, H., Hayashi, T., Kageyama, R., Ohkubo, H., Nakanishi, S., and Murakami, K.,** Cloning and sequence analysis of cDNA for human renin precursor, *Proc. Natl. Acad. Sci. U.S.A.*, 80, 7405, 1983.
19. **Hobart, P. M., Fogliano, M., O'Connor, B. A., Schaefer, I. M., and Chirgwin, J. M.,** Human renin gene: structure and sequence analysis, *Proc. Natl. Acad. Sci. U.S.A.*, 81, 5026, 1984.
20. **Murakami, K.,** Primary and tertiary structure of human renin, *J. Hypertens. Suppl.*, 2, 7, 1984.
21. **Murakami, K., Hirose, S., Miyazaki, H., Imai, T., Hori, H., Hayashi, T., Kageyama, R., Ohkubo, H., and Nakanishi, S.,** Complementary DNA sequences of renin. State-of-the-art review, *Hypertension*, 6, 195, 1984.
22. **Tang, J., Sepulveda, P., Marciniszyn, J., Chen, K. C. S., Huang, W.-Y., Tao, N., Liu, D., and Lanier, J. P.,** Amino-acid sequence of porcine pepsin, *Proc. Natl. Acad. Sci. U.S.A.*, 70, 3437, 1973.
23. **Foltmann, B., Pedersen, V. B., Kaufmann, D., and Wybrandt, G.,** The complete amino acid sequence of prochymosin, *J. Biol. Chem.*, 254, 8447, 1979.
24. **Tang, J., James, M. N., Hsu, I. N., Jenkins, J. A., and Blundell, T. L.,** Structural evidence for gene duplication in the evolution of the acid proteases, *Nature (London)*, 271, 618, 1978.
25. **Andreeva, N. S. and Gustchina, A. E.,** On the supersecondary structure of acid proteases, *Biochem. Biophys. Res. Commun.*, 87, 32, 1979.
26. **Bott, R., Subramanian, E., and Davies, D. R.,** Three-dimensional structure of the complex of the *Rhizopus chinensis* carboxyl proteinase and pepstatin at 2.5-Å resolution, *Biochemistry*, 21, 6956, 1982.
27. **James, M. N. and Sielecki, A. R.,** Stereochemical analysis of peptide bond hydrolysis catalyzed by the aspartic proteinase penicillopepsin, *Biochemistry*, 24, 3701, 1985.
28. **Cumin, F., Le-Nguyen, D., Castro, B., Menard, J., and Corvol, P.,** Comparative enzymatic studies of human renin acting on pure natural or synthetic substrates, *Biochim. Biophys. Acta*, 913, 10, 1987.
29. **Rich, D. H., Salituro, F. G., Holladay, M. W., and Schmidt, P. G.,** Design and discovery of aspartyl protease inhibitors. Mechanistic and clinical implications, in *Conformationally Directed Drug Design. Peptides and Nucleic Acids as Templates or Targets*, Vida, J. A. and Gordon, M., Eds., American Chemical Society, Washington, D.C., 1984, 211.
30. **James, M. N., Sielecki, A., Salituro, F., Rich, D. H., and Hofmann, T.,** Conformational flexibility in the active sites of aspartyl proteinases revealed by a pepstatin fragment binding to penicillopepsin, *Proc. Natl. Acad. Sci. U.S.A.*, 79, 6137, 1982.
31. **Hemmings, A. M., Foundling, S. I., Sibanda, B. L., Wood, S. P., Pearl, L. H., and Blundell, T.,** Energy calculations on aspartic proteinases: human renin, endothiapepsin and its complex with an angiotensinogen fragment analogue, H-142, *Biochem. Soc. Trans.*, 13, 1036, 1985.
32. **Suguna, K., Padlan, E. A., Smith, C. W., Carlson, W. D., and Davies, D. R.,** Binding of a reduced peptide inhibitor to the aspartic proteinase from *Rhizopus chinensis:* implications for a mechanism of action, *Proc. Natl. Acad. Sci. U.S.A.*, 84, 7009, 1987.
33. **Foundling, S. I., Cooper, J., Watson, F. E., Cleasby, A., Pearl, L. H., Sibanda, B. L., Hemmings, A., Wood, S. P., Blundell, T. L., Valler, M. J., Norey, C. G., Kay, J., Boger, J., Dunn, B. M., Leckie, B. J., Jones, D. M., Atrash, B., Hallett, A., and Szelke, M.,** High resolution X-ray analyses of renin inhibitor-aspartic proteinase complexes, *Nature (London)*, 327, 349, 1987.
34. **Sali, A., Veerapandian, B., Cooper, J. B., Foundling, S. I., Hoover, D. J., and Blundell, T. L.,** High-resolution X-ray diffraction study of the complex between endothiapepsin and an oligopeptide inhibitor: the analysis of the inhibitor binding and description of the rigid body shift in the enzyme, *EMBO J.*, 8, 2179, 1989.
35. **Plattner, J. J., Greer, J., Fung, A. K., Stein, H., Kleinert, H. D., Sham, H. L., Smital, J. R., and**

Perun, T. J., Peptide analogues of angiotensinogen. Effect of peptide chain length on renin inhibition, *Biochem. Biophys. Res. Commun.*, 139, 982, 1986.
36. **Sham, H. L., Bolis, G., Stein, H. H., Fesik, S. W., Marcotte, P. A., Plattner, J. J., Rempel, C. A., and Greer, J.,** Renin inhibitors. Design and synthesis of a new class of conformationally restricted analogues of angiotensinogen, *J. Med. Chem.*, 31, 284, 1988.
37. **Hutchins, C. W. and Greer, J.,** (1989).
38. **Craik, C. S., Rutter, W. J., and Fletterick, R.,** Splice junctions: association with variation in protein structure, *Science*, 220, 1125, 1983.
39. **Boger, J., Lohr, N. S., Ulm, E. H., Poe, M., Blaine, E. H., Fanelli, G. M., Lin, T.-Y., Payne, L. S., Schorn, T. W., LaMont, B. I., Vassil, T. C., Stabilito, I. I., Veber, D. F., Rich, D. H., and Bopari, A. S.,** Novel renin inhibitors containing the amino acid statine, *Nature (London)*, 303, 81, 1983.
40. **Boger, J.,** Renin inhibitors. Design of angiotensinogen transition-state analogs containing statine, in *Peptides, Structure and Function. Proceedings of the Eighth American Peptide Symposium*, Hruby, V. J. and Rich, D. J., Eds., Pierce Chemical Co., Rockford, IL, 1983, 569.
41. **Boger, J.,** Renin inhibitors: drug design and molecular modelling, in *Proceedings of the Third SCI-RSC Medicinal Chemistry Symposium; Special Publication No. 55 of the Royal Society of Chemistry*, Lambert, R. W., Eds., London, 1986, 271.
42. **Powers, J. C., Harley, A. D., and Myers, D. V.,** *Acid Proteases — Structure, Function and Biology*, Tang, J., Eds., Plenum Press, New York, 1977, 141.
43. **Burt, S. K., Mackay, D., and Hagler, A. T.,** Theoretical aspects of drug design: molecular mechanics and molecular dynamics, in *Computer-Aided Drug Design. Methods and Applications*, Perun, T. J. and Propst, C. L., Eds., Marcel Dekker, New York, 1989, 55.
44. **Blundell, T., Sibanda, B. L., and Pearl, L.,** Three-dimensional structure, specificity and catalytic mechanism of renin, *Nature (London)*, 304, 273, 1983.
45. **Sibanda, B. L., Blundell, T., Hobart, P. M., Fogliano, M., Bindra, J. S., Dominy, B. W., and Chirgwin, J. M.,** Computer graphics modelling of human renin. Specificity, catalytic activity and intron-exon junctions, *FEBS Lett.*, 174, 102, 1984.
46. **Pearl, L. and Blundell, T.,** The active site of aspartic proteinases, *FEBS Lett.*, 174, 96, 1984.
47. **Jones, T. A.,** A graphics model building and refinement system for macromolecules, *J. Appl. Cryst.*, 11, 268, 1978.
48. **Weiner, P. K. and Kollman, P. A.,** AMBER: assisted model building with energy refinement. A general program for modeling molecules and their interactions, *J. Comp. Chem.*, 2, 287, 1981.
49. **Carlson, W., Karplus, M., and Haber, E.,** Construction of a model for the three-dimensional structure of human renal renin, *Hypertension*, 7, 13, 1985.
50. **Carlson, W., Handschumacher, M., Karplus, M., and Haber, E.,** Studies of the three-dimensional structure of human renin and its inhibitors, *J. Hypertension*, 2, 281, 1984.
51. **Suguna, K., Bott, R. R., Padlan, E. A., Subramanian, E., Sheriff, S., Cohen, G. H., and Davies, D. R.,** Structure and refinement at 1.8 Å resolution of the aspartic proteinase from *Rhizopus chinensis*, *J. Mol. Biol.*, 196, 877, 1987.
52. **Delaney, R., Wong, R. N., Meng, G. Z., Wu, N. H., and Tang, J.,** Amino acid sequence of rhizopuspepsin isozyme pI 5, *J. Biol. Chem.*, 262, 1461, 1987.
53. **Brooks, B., Bruccoleri, R. E., Olafson, B. D., Staden, D. J., Swaminathan, D., and Karplus, M.,** CHARMM: a program for macromolecular energy minimization and dynamics calculations, *J. Comput. Chem.*, 4, 187, 1983.
54. **Carlson, W., Haber, E., Feldmann, R., and Karplus, M.,** A model for the three-dimensional structure of renin, in *Proceedings of the Eighth American Peptide Symposium*, Hruby, V. J. and Rich, D. J., Eds., Pierce Chemical Co., Rockford, IL, 1984, 821.
55. **Akahane, K., Umeyama, H., Nakagawa, S., Moriguchi, I., Hirose, S., Iizuka, K., and Murakami, K.,** Three-dimensional structure of human renin, *Hypertension*, 7, 3, 1985.
56. **James, M. N. and Sielecki, A. R.,** Structure and refinement of penicillopepsin at 1.8 Å resolution, *J. Mol. Biol.*, 163, 299, 1983.
57. **Misono, K. S. and Inagami, T.,** Characterization of the active site of mouse submaxillary gland renin, *Biochemistry*, 19, 2616, 1980.
58. **Bolis, G. and Greer, J.,** Role of computer-aided molecular modeling in the design of novel inhibitors of renin, in *Computer-Aided Drug Design. Methods and Applications*, Perun, T. J. and Propst, C. L., Eds., Marcel Dekker, New York, 1989, 297.
59. **Andreeva, N. S., Zdanov, A. S., Gustchina, A. E., and Fedorov, A. A.,** Structure of ethanol-inhibited porcine pepsin at 2-Å resolution and binding of the methyl ester of phenylalanyl-diiodotyrosine to the enzyme, *J. Biol. Chem.*, 259, 11353, 1984.
60. **Bernstein, F. C., Koetzle, T. F., Williams, G. J., Meyer, E. J., Brice, M. D., Rodgers, J. R., Kennard, O., Shimanouchi, T., and Tasumi, M.,** The Protein Data Bank: a computer-based archival file for macromolecular structures, *J. Mol. Biol.*, 112, 535, 1977.
61. **Dauber, P., Osguthorpe, D., and Hagler, A. T.,** Structure energetics and dynamics of ligand binding to dihydrofolate reductase, *Biochem. Soc. Trans.*, 10, 312, 1982.
62. **Raddatz, E., Schittenhelm, C., and Barnickel, G.,** Computer-graphics methods in pharmaceutical research: visualization of renin-inhibitor complexes, *Kontakte (Darmstadt)*, 3, 1985.

63. **Barnickel, G.,** dissertation, Freie Universität Berlin, 1983.
64. **Abad-Zapatero, C., Rydel, T. J., and Erickson, J.,** Revised 2.3 Å structure of porcine pepsin: evidence for a flexible subdomain, *Proteins,* 7, 1990, in press.
65. **Gilliland, G. L., Winborne, D. L., Nachman, J., and Wlodawer, A.,** Three-dimensional structure of recombinant bovine chymosin at 2.3 Å resolution, *Proteins,* 7, 1990, in press.
66. **Biosym Technologies, Inc.,** San Diego, CA.
67. **Szelke, M., Leckie, B., Hallett, A., Jones, D. M., Sueiras, J., Atrash, B., and Lever, A. F.,** Potent new inhibitors of human renin, *Nature (London),* 299, 555, 1982.
68. **Szelke, M.,** Chemistry of renin inhibitors, in *Aspartic Proteinases and their Inhibitors,* Kostka, V., Ed., Walter de Gruyter, Berlin, 1985, 421.
69. **Novotny, J., Handschumacher, M., Haber, E., Bruccoleri, R. E., Carlson, W. D., Fanning, D. W., Smith, J. A., and Rose, G. D.,** Antigenic determinants in proteins coincide with surface regions accessible to large probes (antibody domains), *Proc. Natl. Acad. Sci. U.S.A.,* 83, 226, 1986.
70. **Evin, G., Galen, F.-X., Carlson, W. D., Handschumacher, M., Novotny, J., Bouhnik, J., Menard, J., Corvol, P., and Haber, E.,** Characterization of five epitopes of human renin from a computer model, *Biochemistry,* 27, 156, 1988.
71. **Bouhnik, J., Galen, F.-X., Menard, J., Corvol, P., Seyer, R., Fehrentz, J.-A., Nguyen, D. L., Fulcrand, P., and Castro, B.,** Production and characterization of human renin antibodies with region-oriented synthetic peptides, *J. Biol. Chem.,* 262, 2913, 1987.
72. **Fehrentz, J. A., Heitz, A., Seyer, R., Fulcrand, P., Devilliers, R., Castro, B., Heitz, F., and Carelli, C.,** Peptides mimicking the flap of human renin: synthesis, conformation, and antibody recognition, *Biochemistry,* 27, 4071, 1988.
73. **Fa, L. C., Fehrentz, J.-A., Heitz, A., Dung, L. N., Castro, B., Heitz, F., Carelli, C., Galen, F.-X., and Corvol, P.,** Synthesis, conformation, and antibody recognition of peptides built of the sequence of the flap of human renin, *Tetrahedron,* 44, 675, 1988.
74. **Yamauchi, T., Nagahama, M., Hori, H., and Murakami, K.,** Functional characterization of Asp-317 mutant of human renin expressed in COS cells, *FEBS Lett.,* 230, 205, 1988.
75. **Green, D. W., Aykent, S., Gierse, J. K., and Zupec, M. E.,** Substrate specificity of recombinant human renal renin: effect of histidine in the P2 subsite on pH dependence, *Biochemistry,* 29, 3126, 1990.
76. **Sawyer, T. K., Pals, D. T., Mao, B., Maggiora, L. L., Staples, D. J., deVaux, A. E., Schostarez, H. J., Kinner, J. H., and Smith, C. W.,** Structure-conformation-activity relationships of renin inhibitory peptides having P1-P1′ Xaa-psi[CH2NH]Yaa substitutions: molecular modeling and crystallography studies, *Tetrahedron,* 44, 661, 1988.
77. **Sawyer, T. K., Pals, D. T., Mao, B., Staples, D. J., deVaux, A. E., Maggiora, L. L., Affholter, J. A., Kati, W., Duchamp, D., Hester, J. B., Smith, C. W., Saneii, H. H., Kinner, J., Handschumacher, M., and Carlson, W.,** Design, structure-activity, and molecular modeling studies of potent renin inhibitory peptides having N-terminal Nin-For-Trp (Ftr): angiotensinogen congeners modified by P1-P1′ Phe-Phe, Sta, Leu-psi[CH(OH)CH2]Val or Leu-psi[CH2NH]Val substitutions, *J. Med. Chem.,* 31, 18, 1988.
78. **Sawyer, T. K., Pals, D. T., Smith, C. W., Saneii, H. H., Epps, D. E., Duchamp, D. J., Hester, J. B., TenBrink, R. E., Stapley, D. J., deVaux, A. E., Affholter, J. A., Skala, G. F., Kati, W. M., Lawson, J. A., Schuette, M. R., Kamdar, B. V., and Emmert, D. E.,** "Transition state" substituted renin inhibitory peptides: structure-conformation-activity studies on Nin-formyl-Trp and Trp modified congeners, in *Peptides, Structure and Function. Proceedings of the Ninth American Peptide Symposium,* Deber, C. M., Hruby, V. J., and Kopple, K. D., Eds., Pierce Chemical Co., Rockford, IL, 1985, 729.
79. **Hui, K. Y., Carlson, W. D., Bernatowicz, M. S., and Haber, E.,** Analysis of structure-activity relationships in renin substrate analogue inhibitory peptides, *J. Med. Chem.,* 30, 1287, 1987.
80. **Epps, D. E., Mao, B., Staples, D. J., and Sawyer, T. K.,** Structure-conformation relationships of synthetic peptide inhibitors of human renin studied by resonance energy transfer and molecular modeling, *Int. J. Pept. Protein Res.,* 31, 22, 1988.
81. **Carlson, W. D., Handschumacher, M., Summers, N., Karplus, M., and Haber, E.,** Models for the three-dimensional structure of renin inhibitors bound in the active site of human renin: an analysis of the properties that produce tight binding, *J. Cardiovasc. Pharmacol.,* 10 (Suppl. 7), S91, 1987.
82. **Matsueda, R., Yabe, Y., Kogen, H., Higashida, S., Koike, H., Iijima, Y., Kokubu, T., Hiwada, K., Murakami, E., and Imamura, Y.,** Short chain peptide inhibitors of human renin, *Chem. Lett.,* 1041, 1985.
83. **Hanson, G. J., Baran, J. S., Lindberg, T., Walsh, G. M., Papaioannou, S. E., Babler, M., Bittner, S. E., Yang, P. C., and Dal Corobbo, M.,** Dipeptide glycols: a new class of renin inhibitors, *Biochem. Biophys. Res. Commun.,* 132, 155, 1985.
84. **Luly, J. R., BaMaung, N., Soderquist, J., Fung, A. K., Stein, H., Kleinert, H. D., Marcotte, P. A., Egan, D. A., Bopp, B., Merits, I., Bolis, G., Greer, J., Perun, T. J., and Plattner, J. J.,** Renin inhibitors. Dipeptide analogues of angiotensinogen utilizing a dihydroxyethylene transition-state mimic at the scissile bond to impart greater inhibitory potency, *J. Med. Chem.,* 31, 2264, 1988.

85. **Rosenberg, S. H., Dellaria, J. F., Kempf, D. J., Hutchins, C. W., Woods, K. W., Maki, R. G., de Lara, E., Spina, K. P., Stein, H. H., Cohen, J., Baker, W. R., Plattner, J. J., Kleinert, H. D., and Perun, T. J.,** Potent, low molecular weight renin inhibitors containing a C-terminal heterocycle: hydrogen bonding at the active site, *J. Med. Chem.*, 33, 1582, 1990.
86. **Hanson, G. J., Baran, J. S., Lowrie, H. S., Sarussi, S. J., Yang, P. C., Babler, M., Bittner, S. E., Papaioannou, S. E., and Walsh, G. M.,** Enhanced potency dipeptide glycol renin inhibitors: studies in vitro and in the conscious rhesus, *Biochem. Biophys. Res. Commun.*, 146, 959, 1987.
87. **Hanson, G. J., Baran, J. S., Clare, M., Williams, K., Babler, M., Bittner, S. E., Russell, M. A., Papaioannou, S. E., Yang, P.-C., and Walsh, G. M.,** Orally active renin inhibitors containing a novel aminoglycol dipeptide (Leu-Val) mimetic, in *Peptides. Chemistry, Structure and Biology. Proceedings of the Eleventh American Peptide Symposium*, Rivier, J. E. and Marshall, G. R., Eds., ESCOM Science Publishers, Leiden, The Netherlands, 1990, 396.
88. **Thaisrivongs, S., Pals, D. T., Kroll, L. T., Turner, S. R., and Han, F.-S.,** Renin inhibitors. Design of angiotensinogen transition-state analogues containing novel (2R,3R,4R,5S)-5-amino-3,4-dihydroxy-2-isopropyl-7-methyloctanoic acid, *J. Med. Chem.*, 30, 976, 1987.
89. **Plattner, J. J., Marcotte, P. A., Kleinert, H. D., Stein, H. H., Greer, J., Bolis, G., Fung, A. K. L., Bopp, B. A., Luly, J. R., Sham, H. L., Kempf, D. J., Rosenberg, S. H., Dellaria, J. F., De, B., Merits, I., and Perun, T. J.,** Renin inhibitors. Dipeptide analogues of angiotensinogen utilizing a structurally modified phenylalanine residue to impart proteolytic stability, *J. Med. Chem.*, 31, 2277, 1988.
90. **Thaisrivongs, S., Pals, D. T., Turner, S. R., and Kroll, L. T.,** Conformationally constrained renin inhibitory peptides: gamma-lactam-bridged dipeptide isostere as conformational restriction, *J. Med. Chem.*, 31, 1369, 1988.
91. **Thaisrivongs, S., Pals, D. T., Harris, D. W., Kati, W. M., and Turner, S. R.,** Design and synthesis of a potent and specific renin inhibitor with a prolonged duration of action in vivo, *J. Med. Chem.*, 29, 2088, 1986.
92. **de Laszlo, S. E., Bush, B. L., Doyle, J. J., Greenlee, W. J., Hangauer, D. G., Halgren, T. A., Lynch, R. J., Schorn, T. W., and Siegl, P. K. S.,** The synthesis and use of 3-amino-4-phenyl-2-piperidones and 4-amino-2-benzazepine-3-ones as conformationally restricted phenylalanine isosteres in renin inhibitors, in *Peptides. Chemistry, Structure and Biology. Proceedings of the Eleventh American Peptide Symposium*, Rivier, J. E. and Marshall, G. R., Eds., ESCOM Science Publishers B.V., Leiden, The Netherlands, 1990, 409.
93. **Lunney, E. A. and Humblet, C. C.,** Comparative molecular modeling analyses of endothiapepsin complexes as renin model templates, in *Peptides. Chemistry, Structure and Biology. Proceedings of the Eleventh American Peptide Symposium*, Rivier, J. E. and Marshall, G. R., Eds., ESCOM Science Publishers B.V., Leiden, The Netherlands, 1990, 387.
94. **Kaltenbronn, J. S., Hudspeth, J. P., Lunney, E. A., Nicolaides, E. D., Repine, J. T., Roark, W. H., Stier, M. A., Tinney, F. J., Woo, P. K. W., and Essenburg, A. D.,** Isostere containing renin inhibitors, in *Peptides. Chemistry, Structure and Biology. Proceedings of the Eleventh American Peptide Symposium*, Rivier, J. E. and Marshall, G. R., Eds., ESCOM Science Publishers B.V., Leiden, The Netherlands, 1990, 404.
95. **Luly, J. R., Bolis, G., BaMaung, N., Soderquist, J., Dellaria, J. F., Stein, H., Cohen, J., Perun, T. J., Greer, J., and Plattner, J. J.,** New inhibitors of human renin that contain novel Leu-Val replacements. Examination of the P1 site, *J. Med. Chem.*, 31, 532, 1988.
96. **Boger, J., Payne, L. S., Perlow, D. S., Lohr, N. S., Poe, M., Blaine, E. H., Ulm, E. H., Schorn, T. W., LaMont, B. I., Lin, T.-Y., Kawai, M., Rich, D. H., and Veber, D. F.,** Renin inhibitors. Syntheses of subnanomolar, competitive, transition-state analogue inhibitors containing a novel analogue of statine, *J. Med. Chem.*, 28, 1779, 1985.
97. **Bock, M. G., DiPardo, R. M., Evans, B. E., Freidinger, R. M., Rittle, K. E., Payne, L. S., Boger, J., Whitter, W. L., LaMont, B. I., Ulm, E. H., Blaine, E. H., Schorn, T. W., and Veber, D. F.,** Renin inhibitors containing hydrophilic groups. Tetrapeptides with enhanced aqueous solubility and nanomolar potency, *J. Med. Chem.*, 31, 1918, 1988.
98. **Akahane, K., Kamijo, T., Iizuka, K., Taguchi, T., Kobayashi, Y., Kiso, Y., and Umeyama, H.,** Structure-activity relationship of fluorine-containing renin inhibitory peptides based upon the tertiary structure of human renin, *Chem. Pharm. Bull.*, 36, 3447, 1988.
99. **Rekker, R. F. and deKort, H. M.,** The hydrophobic fragment constant; an extension to a 1000 data point set, *Eur. J. Med. Chem.*, 14, 479, 1979.
100. **Veber, D. F., Bock, M. G., Brady, S. F., Ulm, E. H., Cochran, D. W., Smith, G. M., LaMont, B. I., Dipardo, R. M., Poe, M., Freidinger, R. M., Evans, B. E., and Boger, J.,** Renin inhibitors containing 2-substituted statine, *Biochem. Soc. Trans.*, 12, 956, 1984.
101. **Stein, H., Cohen, J., Tricarico, K., Sham, H., Rempel, C., Perun, T., and Plattner, J.,** Proteolytic and species specificities of substituted statine-containing renin inhibitors, *Fed. Proc.*, 45, 869, 1986.
102. **Iizuka, K., Kamijo, T., Kubota, T., Akahane, K., Umeyama, H., and Kiso, Y.,** New human renin inhibitors containing an unnatural amino acid, norstatine, *J. Med. Chem.*, 31, 701, 1988.

103. **Bolis, G., Fung, A. K. L., Greer, J., Kleinert, H. D., Marcotte, P. A., Perun, T. J., Plattner, J. J., and Stein, H. H.,** Renin inhibitors. Dipeptide analogues of angiotensinogen incorporating transition-state, nonpeptidic replacements at the scissile bond, *J. Med. Chem.*, 30, 1729, 1987.
104. **Nakaie, C. R., Oliveira, M. C. F., Juliano, L., and Paiva, A. C. M.,** Inhibition of renin by conformationally restricted analogues of angiotensinogen, *Biochem. J.*, 205, 43, 1982.
105. **Nakaie, C. R., Oliveria, M. C. F., Juliano, L., Pesquero, J. L., and Paiva, A. C. M.,** Renin inhibition by linear and cyclic analogs of the angiotensinogen-(6-11) sequence, in *Peptides, Structure and Function. Proceedings of the Eighth American Peptide Symposium,* Hruby, V. J. and Rich, D. H., Eds., Pierce Chemical Co., Rockford, IL, 1983, 595.
106. **Nakaie, C. R., Pesquero, J. L., Oliveira, M. C. F., Juliano, L., and Paiva, A. C. M.,** Renin inhibition by linear and conformationally restricted analogs of renin substrate, in *Peptides, Structure and Function. Proceedings of the Ninth American Peptide Symposium,* Deber, C. M., Hruby, V. J., and Kopple, K. D., Eds., Pierce Chemical Co., Rockford, IL, 1985, 755.
107. **Sham, H. L., Bolis, G., Stein, H. H., Fesik, S. W., Marcotte, P. A., Plattner, J. J., Rempel, C. A., and Greer, J.,** Renin inhibitors. Design and synthesis of a new class of conformationally restricted analogues of angiotensinogen, *J. Med. Chem.*, 31, 284, 1988.
108. **Fesik, S. W., Bolis, G., Sham, H. L., and Olejniczak, E. T.,** Structure refinement of a cyclic peptide from two-dimensional NMR data and molecular modeling, *Biochemistry,* 26, 1851, 1987.
109. **Goodford, P. J.,** A computational procedure for determining energetically favorable binding sites on biologically important macromolecules, *J. Med. Chem.*, 28, 849, 1985.
110. **VanDrie, J. H., Weininger, D., and Martin, Y. C.,** ALADDIN: an integrated tool for computer-assisted molecular design and pharmacophore recognition from geometric, steric, and substructure searching of three-dimensional molecular structures, *J. Computer-Aided Mol. Des.*, 3, 225, 1989.
111. **Bartlett, P. A., Shea, G. T., Telfer, S. J., and Waterman, S.,** CAVEAT: a program to facilitate the structure-derived design of biologically active molecules, in *Chemical and Biological Problems in Molecular Recognition,* Roberts, S. M., Ley, S. V., and Campbell, M. M., Eds., Royal Society of Chemistry, London, in press.
112. **Schechter, I. and Berger, A.,** On the size of the active site in proteases. I. Papain, *Biochem. Biophys. Res. Commun.*, 27, 157, 1967.
113. **Barkholt, V.,** Amino acid sequence of endothiapepsin. Complete primary structure of the aspartic protease from *Endothia parasitica, Eur. J. Biochem.*, 167, 327, 1987.
114. **Shewale, J. G. and Tang, J.,** Amino acid sequence of porcine spleen cathepsin D, *Proc. Natl. Acad. Sci. U.S.A.*, 81, 3703, 1984.
115. **Bernstein, F. C., Koetzle, T. F., Williams, G. J., Meyer, E. J., Brice, M. D., Rodgers, J. R., Kennard, O., Shimanouchi, T., and Tasumi, M.,** The protein data bank: a computer-based archival file for macromolecular structures, *Arch. Biochem. Biophys.*, 185, 584, 1978.